

A search for new physics in dijet mass and angular distributions in pp collisions at $\sqrt{s} = 7$ TeV measured with the ATLAS detector

The ATLAS Collaboration

New Journal of Physics **13** (2011) 053044 (44pp)

Received 20 March 2011

Published 24 May 2011

Online at <http://www.njp.org/>

doi:10.1088/1367-2630/13/5/053044

Abstract. A search for new interactions and resonances produced in LHC proton–proton (pp) collisions at a centre-of-mass energy $\sqrt{s} = 7$ TeV was performed with the ATLAS detector. Using a dataset with an integrated luminosity of 36 pb^{-1} , dijet mass and angular distributions were measured up to dijet masses of ~ 3.5 TeV and were found to be in good agreement with Standard Model predictions. This analysis sets limits at 95% CL on various models for new physics: an excited quark is excluded for mass between 0.60 and 2.64 TeV, an axigluon hypothesis is excluded for axigluon masses between 0.60 and 2.10 TeV and quantum black holes are excluded in models with six extra space–time dimensions for quantum gravity scales between 0.75 and 3.67 TeV. Production cross section limits as a function of dijet mass are set using a simplified Gaussian signal model to facilitate comparisons with other hypotheses. Analysis of the dijet angular distribution using a novel technique simultaneously employing the dijet mass excludes quark contact interactions with a compositeness scale Λ below 9.5 TeV.

Contents

1. Introduction	2
2. Kinematics and angular distributions	3
3. The ATLAS detector and event selection	5
3.1. The detector and trigger requirements	5
3.2. Common event selection	5
4. Theoretical models and Monte Carlo (MC) simulations	6
4.1. Quantum chromodynamics (QCD) production	6
4.2. Models for new physics phenomena	7
5. Search for dijet resonances	8
5.1. The dijet mass distribution	8
5.2. Exclusion limits using the dijet mass	10
5.3. Limits on excited quark production	10
5.4. Limits on axigluon production	12
5.5. Limits on quantum black hole (QBH) production	12
5.6. Limits on Randall–Sundrum (RS) graviton production	12
5.7. Simplified Gaussian model limits	13
6. Angular distribution analyses	14
6.1. Systematic and statistical uncertainties	15
6.2. Observed χ and $F_\chi(m_{jj})$ distributions	16
6.3. Exclusion limits from likelihood ratios	17
6.4. Limits on quark contact interactions	18
6.5. Limits on excited quark production	19
6.6. Limits on new physics for additive signals	20
6.7. Limits on QBH production	21
7. Conclusion	23
Acknowledgments	24
References	42

1. Introduction

The search for new phenomena in particle interactions is perhaps most exciting when new vistas are opened up by significant increases in experimental sensitivity, either by collecting larger samples of data or by entering kinematic regimes never before explored. Searches are particularly compelling when one can do both, as has recently become the case in the first studies of proton–proton (pp) collisions at a centre-of-mass (CM) energy of 7 TeV produced at the CERN Large Hadron Collider (LHC). We report on a search for massive objects and new interactions using a sample of 36 pb^{-1} of integrated luminosity observed by the ATLAS detector.

This analysis focuses on those final states where two very energetic jets of particles are produced with large transverse momentum (p_T) transfer. These $2 \rightarrow 2$ scattering processes are well described within the Standard Model (SM) by perturbative quantum chromodynamics (QCD), the quantum field theory of strong interactions. However, there could be additional

contributions from the production of a new massive particle that then decays into a dijet final state, or the rate could be enhanced through a new force that only manifests itself at very large CM energies.

One can perform sensitive searches for new phenomena by studying both the dijet invariant mass, m_{jj} , and the angular distributions of energetic jets relative to the beam axis, usually described by the polar scattering angle in the two-parton CM frame, θ^* . QCD calculations predict that high- p_T dijet production is dominated by t -channel gluon exchange, leading to rapidly falling m_{jj} distributions and angular distributions that are peaked at $|\cos \theta^*|$ close to 1. By contrast, models of new processes characteristically predict angular distributions that would be more isotropic than those of QCD. Discrepancies from the predicted QCD behaviour would be evidence for new physics. This analysis focuses on a study of dijet mass and angular distributions, which have been shown by previous studies [1–9] to be sensitive to new processes. These dijet variables are well suited for searches employing early LHC data. The dijet mass analyses can be performed using data-driven background estimates, while the angular analyses can be designed to have reduced sensitivity to the systematic uncertainties associated with the jet energy scale (JES) and integrated luminosity.

Following the first ATLAS studies of massive dijet events with 0.3 pb^{-1} [5] and 3.1 pb^{-1} [6], the full 2010 data set has increased statistical power by more than an order of magnitude, and we have made several improvements to the analysis. A variety of models of new physics have been tested and the angular distributions have been analysed using a new technique that finely bins the data in dijet mass to maximize the sensitivity of the search to both resonant and non-resonant phenomena. We set limits on a number of models and provide cross section limits using a simplified Gaussian signal model to facilitate tests of other hypotheses that we have not considered.

Section 2 describes the kinematic variables we used in this search. Section 3 describes the detector and the data sample, as well as the common event selection criteria used in the studies reported here. Section 4 describes the theoretical models employed, including the procedures used to account for detector effects. Section 5 describes the search for resonance and threshold phenomena using the dijet invariant mass. Section 6 describes the studies employing the angular distributions as a function of the invariant mass of the dijet system. Section 7 summarizes our results.

2. Kinematics and angular distributions

This analysis is focused on those pp collisions that produce two high-energy jets recoiling back-to-back in the partonic CM frame to conserve momentum relative to the beamline. The dijet invariant mass, m_{jj} , is defined as the mass of the two highest p_T jets in the event. The scattering angle θ^* distribution for $2 \rightarrow 2$ parton scattering is predicted by QCD in the parton CM frame, which is in practice moving along the beamline due to the different momentum fractions (Bjorken x) of one incoming parton relative to the other. The rapidity of each jet is therefore a natural variable for the study of these systems, $y \equiv \frac{1}{2} \ln\left(\frac{E+p_z}{E-p_z}\right)$, where E is the jet energy and p_z is the z -component of the jet's momentum¹. The variable y transforms under a

¹ The ATLAS coordinate system is a right-handed Cartesian system with the x -axis pointing to the centre of the LHC ring, the z -axis following the counter-clockwise beam direction and the y -axis directed upwards. The polar angle θ refers to the z -axis, and ϕ is the azimuthal angle about the z -axis. Pseudo-rapidity is defined as $\eta \equiv -\ln \tan(\theta/2)$ and is a good approximation to rapidity as the particle mass approaches zero.

Lorentz boost along the z -direction as $y \rightarrow y - y_B = y - \tanh^{-1}(\beta_B)$, where β_B is the velocity of the boosted frame, and y_B is its rapidity boost.

We use the m_{jj} spectrum as a primary tool to search for new particles that would be observed as resonances. The m_{jj} spectrum is also sensitive to other phenomena, such as threshold enhancements or the onset of new interactions at multi-TeV mass scales in our current data sample. We bin the data in m_{jj} choosing bin-widths that are consistent with the detector resolution as a function of mass so that binning effects do not limit our search sensitivity.

We employ the dijet angular variable χ derived from the rapidities of the two highest p_T jets, y_1 and y_2 . For a given scattering angle θ^* , the corresponding rapidity in the parton CM frame (in the massless particle limit) is $y^* = \frac{1}{2} \ln\left(\frac{1+|\cos\theta^*|}{1-|\cos\theta^*|}\right)$. We determine y^* and y_B from the rapidities of the two jets using $y^* = \frac{1}{2}(y_1 - y_2)$ and $y_B = \frac{1}{2}(y_1 + y_2)$. The variable y^* is used to determine the partonic CM angle θ^* and to define $\chi \equiv \exp(|y_1 - y_2|) = \exp(2|y^*|)$. As noted in previous studies, the utility of the χ variable arises because the χ distributions associated with final states produced via QCD interactions are relatively flat compared with the distributions associated with new particles or interactions that typically peak at low values of χ .

In a previous dijet angular distributions analysis [6], a single measure of isotropy based on y^* intervals was introduced. This measure, F_χ , is the fraction of dijets produced centrally versus the total number of observed dijets for a specified dijet mass range. We extend this to a measure that is finely binned in dijet mass intervals:

$$F_\chi \left([m_{jj}^{\min} + m_{jj}^{\max}] / 2 \right) \equiv \frac{N_{\text{events}}(|y^*| < 0.6, m_{jj}^{\min}, m_{jj}^{\max})}{N_{\text{events}}(|y^*| < 1.7, m_{jj}^{\min}, m_{jj}^{\max})}, \quad (1)$$

where N_{events} is the number of candidate events within the y^* interval and in the specified m_{jj} range. The interval $|y^*| < 0.6$ defines the central region where we expect to be most sensitive to new physics and corresponds to the angular region $\chi < 3.32$, while $|y^*| < 1.7$ extends the angular range to $\chi < 30.0$, where QCD processes dominate. This new observable, $F_\chi(m_{jj})$, is defined using the same fine m_{jj} binning used in analysis of the m_{jj} spectrum. We also employ the variable F_χ to denote the ratio in equation (1) for dijet masses above 2 TeV. Our studies have shown that the $F_\chi(m_{jj})$ distribution is sensitive to mass-dependent changes in the rate of centrally produced dijets.

Jets are reconstructed using the infrared-safe anti- k_t jet clustering algorithm [10, 11] with the distance parameter $R = 0.6$. The inputs to this algorithm are clusters of calorimeter cells defined by energy depositions significantly above the measured noise. Jet four-momenta are constructed by the vectorial addition of cell clusters, treating each cluster as an (E, \vec{p}) four-vector with zero mass. The jet four-momenta are then corrected as a function of η and p_T for various effects, the largest of which are the hadronic shower response and detector material distributions. This is done using a calibration scheme based on Monte Carlo (MC) studies including full detector simulation and validated with extensive test-beam studies [12] and collision data [13–15].

The measured distributions include corrections for the JES but are not unfolded to account for resolution effects. These distributions are compared to theoretical predictions processed through a full detector simulation software.

3. The ATLAS detector and event selection

3.1. The detector and trigger requirements

The ATLAS detector [16] is instrumented over almost the entire solid angle around the pp collision point with layers of tracking detectors, calorimeters and muon chambers. Jet measurements are made using a finely segmented calorimeter system designed to efficiently detect the high-energy jets that are the focus of the study.

The electromagnetic (EM) calorimeter consists of an accordion-shaped lead absorber over the region $|\eta| < 3.2$, using liquid argon (LAr) as the active medium to measure the energy and geometry of the showers arising from jets. The measurement of hadronic energy flow in the range $|\eta| < 1.7$ is complemented by a sampling calorimeter made of steel and scintillating tiles. In the end-cap region $1.5 < |\eta| < 3.2$, hadronic calorimeters consisting of a steel absorber and a LAr active medium match the outer $|\eta|$ limits of the EM calorimeters. To complete the η coverage to $|\eta| < 4.9$, the LAr forward calorimeters provide both EM and hadronic energy measurements. The calorimeter (η, ϕ) granularities are $\sim 0.1 \times 0.1$ for the hadronic calorimeters up to $|\eta| < 2.5$ and then 0.2×0.2 up to $|\eta| < 4.9$. The EM calorimeters feature a finer readout granularity varying by layer, with cells as small as 0.025×0.025 extending over $|\eta| < 2.5$.

The inner tracking detector (ID) covers the range $|\eta| < 2.5$, and consists of a silicon pixel detector, a silicon microstrip detector (SCT) and, at $|\eta| < 2.0$, a transition radiation tracker (TRT). The ID is surrounded by a thin superconducting solenoid providing a 2T magnetic field.

ATLAS has a three-level trigger system, with the first level trigger (L1) being custom-built hardware and the two higher level triggers (HLT) being realized in software. The triggers employed in this study selected events that had at least one large transverse energy deposition, with the transverse energy threshold varying over the period of the data-taking as the instantaneous luminosity of the LHC pp collisions rose.

The primary first-level jet trigger used in the resonance analysis had an efficiency of $> 99\%$ for events with dijet masses $m_{jj} > 500$ GeV. This is illustrated in figure 1 where we show the measured trigger efficiency as a function of m_{jj} . After applying the full event selection from the resonance analysis (except the m_{jj} cut) we compute the fraction of events passing a reference trigger which also pass our analysis trigger. The reference trigger is an inclusive jet trigger that was fully efficient for $p_T > 80$ GeV, while our event selection already requires $p_T > 150$ GeV to guarantee full efficiency of the reference trigger. Thus, we efficiently identify events for the dijet resonance analysis at $m_{jj} > 500$ GeV.

In order to have uniform acceptance for the angular distribution analysis, additional lower- p_T triggers were used for different angular and mass regions. We verified that these triggers provided uniform acceptance as a function of χ for the dijet mass intervals in which they were employed. Because these lower threshold triggers sampled only a subset of the pp collisions at higher instantaneous luminosity, the effective integrated luminosity collected for dijet masses between 500 and 800 GeV was 2.2 pb^{-1} and that between 800 and 1200 GeV was 9.6 pb^{-1} in the dijet angular distribution analysis. Above 1200 GeV, the same trigger is used for the resonance and angular analyses, and the full 36 pb^{-1} are used for both analyses.

3.2. Common event selection

Events are required to have at least one primary collision vertex defined by more than four charged-particle tracks. Events with at least two jets are retained if the highest p_T jet (the

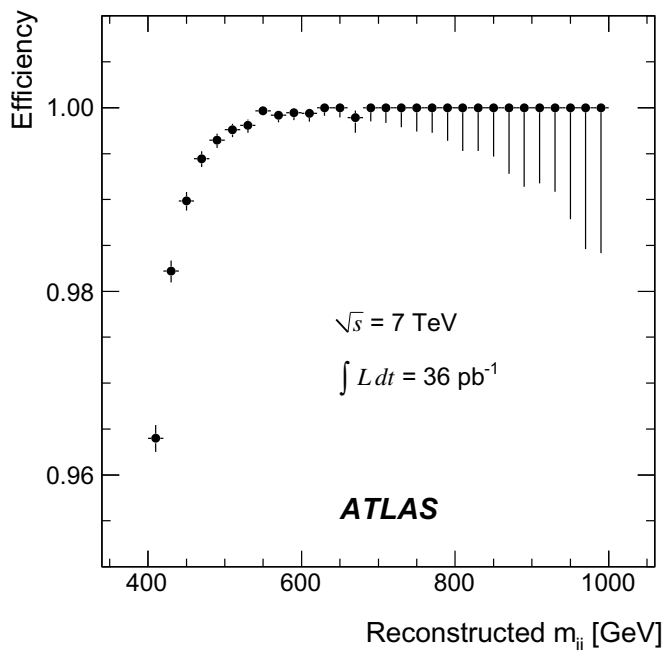


Figure 1. The efficiency of passing the primary first-level trigger as a function of the dijet invariant mass, m_{jj} . The uncertainties are statistical.

‘leading’ jet) satisfies $p_T^{j1} > 60$ GeV and the next-to-leading jet satisfies $p_T^{j2} > 30$ GeV. The asymmetric thresholds avoid suppression of events where a third jet has been radiated, while the 30 GeV threshold ensures that reconstruction is fully efficient for both leading jets. Events containing a poorly measured jet [17] with $p_T > 15$ GeV are vetoed to avoid cases where such a jet would cause incorrect identification of the two leading jets. This criterion rejects less than 0.6% of the events. The two leading jets are required to satisfy quality criteria that ensure that they arise from in-time energy deposition.

Further requirements are made on the jets in order to optimize the analysis of the dijet mass spectrum and angular distributions, as described in sections 5 and 6.

4. Theoretical models and Monte Carlo (MC) simulations

The MC signal samples used for the analysis have been produced with a variety of event generators. We have employed several of the most recent parton distribution functions (PDFs) so that we consistently match the orders of the matrix element calculations implemented in the different MC generators when we calculate QCD predictions, and to be conservative in the calculation of expected new physics signals (all new physics signals are calculated only to leading order (LO)).

4.1. Quantum chromodynamics (QCD) production

The angular distribution analyses required a prediction for the angular distribution arising from QCD production. MC samples modelling QCD dijet production were created with the PYTHIA 6.4.21 event generator [18] and the ATLAS MC09 parameter tune [19], using the

modified leading-order MRST2007 [20] PDF (MRST2007LO*). The generated events were passed through the detailed simulation of the ATLAS detector [21], which uses the GEANT4 package [22] for the simulation of particle transport, interactions, and decays, to incorporate detector effects. The simulated events were then reconstructed in the same way as the data to produce predicted dijet mass and angular distributions that can be compared with the observed distributions.

Bin-by-bin correction factors (K -factors) have been applied to the angular distributions derived from MC calculations to account for next-to-leading order (NLO) contributions. These K -factors were derived from dedicated MC samples and are defined as the ratio $\text{NLO}_{\text{ME}}/\text{PYT}_{\text{SHOW}}$. The NLO_{ME} sample was produced using matrix elements in NLOJET++ [23–25] with the NLO PDF from CTEQ6.6 [26]. The PYT_{SHOW} sample was produced with the PYTHIA generator restricted to LO matrix elements and parton showering using the MRST2007LO* PDF.

The angular distributions generated with the full PYTHIA calculation include various non-perturbative effects such as multiple parton interactions and hadronization. The K -factors defined above were designed to retain these effects while adjusting for differences in the treatment of perturbative effects. We multiplied the full PYTHIA predictions of angular distributions by these binwise K -factors to obtain a reshaped spectrum that includes corrections originating from NLO matrix elements. Over the full range of χ , the K -factors change the normalized angular distributions by up to 6%, with little variability from one mass bin to the other.

The QCD predictions used for comparison with the measured angular distributions in this paper are the product of the two-step procedure described above.

4.2. Models for new physics phenomena

MC signal events for a benchmark beyond-the-SM resonant process were generated using the excited-quark ($qg \rightarrow q^*$) production model [27, 28]. The excited quark q^* was assumed to have spin-1/2 and quark-like couplings, relative to those of the SM $SU(2)$, $U(1)$ and $SU(3)$ gauge groups, of $f = f' = f_s = 1$, respectively. The compositeness scale (Λ) was set to the q^* mass. Signal events were produced using the PYTHIA event generator with the MRST2007LO* PDF and with the renormalization and factorization scales set to the mean p_T of the two leading jets. We also used the PYTHIA MC generator to decay the excited quarks to all possible SM final states, which are dominantly qg but also qW , qZ and $q\gamma$. The MC samples were produced using the ATLAS MC09 parameter tune.

We also considered two other models of new physics that generate resonant signatures: axigluons and Randall–Sundrum (RS) gravitons. The axigluon interaction [29–31] is described by the Lagrangian

$$\mathcal{L}_{Aq\bar{q}} = g_{\text{QCD}} \bar{q} A_{\mu}^a \frac{\lambda^a}{2} \gamma^{\mu} \gamma_5 q. \quad (2)$$

The parton-level events were generated using the CALCHEP MC package [32] with MRST2007LO* PDF. We used a PYTHIA MC calculation to model the production and decays of an RS graviton [33, 34] of a given mass. We performed this calculation with the dimensionless coupling $\kappa/\bar{M}_{\text{Pl}} = 0.1$, where \bar{M}_{Pl} is the reduced Planck mass, to set limits comparable to other searches [7, 35].

For non-resonant new phenomena, we used a benchmark quark contact interaction (CI) as the beyond-the-SM process. This models the onset of kinematic properties that characterize quark compositeness: the hypothesis that quarks are composed of more fundamental particles. The model Lagrangian is a four-fermion contact interaction [36–38] whose effect appears below or near a characteristic energy scale Λ . While a number of contact terms are possible, the Lagrangian in standard use since 1984 [36] is the single (isoscalar) term:

$$\mathcal{L}_{qqqq}(\Lambda) = \frac{\xi g^2}{2\Lambda^2} \bar{\Psi}_q^L \gamma^\mu \Psi_q^L \bar{\Psi}_q^L \gamma_\mu \Psi_q^L, \quad (3)$$

where $g^2/4\pi = 1$ and the quark fields Ψ_q^L are left-handed. The full Lagrangian used for hypothesis testing is then the sum of $\mathcal{L}_{qqqq}(\Lambda)$ and the QCD Lagrangian. The relative phase of these terms is controlled by the interference parameter, ξ , which is set for destructive interference ($\xi = +1$) in the current analysis. Previous analyses [3] showed that the choice of constructive ($\xi = -1$) or destructive ($\xi = +1$) interference changed exclusion limits by $\sim 1\%$. MC samples were created by a PYTHIA 6.4.21 calculation using this Lagrangian, with each sample corresponding to a distinct value of Λ .

As another example of non-resonant new physics phenomena, we considered quantum black holes (QBH) [39, 40], by which we mean any quantum gravitational effect that produces events containing dijets. We used the BLACKMAX black hole event generator [41] to simulate the simplest two-body final state scenario describing the production and decay of a QBH for a given fundamental quantum gravity scale M_D . These would appear as a threshold effect that also depends on the number of extra space–time dimensions.

Previous ATLAS jet studies [42] have shown that the use of different event generators and models for non-perturbative behaviour has a negligible effect on the observables in the kinematic region we are studying. All of the MC signal events were modelled with the full ATLAS detector simulation.

5. Search for dijet resonances

We make a number of additional selection requirements on the candidate events to optimize the search for effects in the dijet mass distribution. Each event is required to have its two highest- p_T jets satisfy $|\eta_j| < 2.5$ with $|\Delta\eta_{jj}| < 1.3$. In addition, the leading jet must satisfy $p_T^{j_1} > 150$ GeV and m_{jj} must be greater than 500 GeV. These criteria have been shown, based on studies of expected signals and QCD background, to efficiently optimize the signal-to-background in the sample. There are 98 651 events meeting these criteria.

5.1. The dijet mass distribution

In order to develop a data-driven model of the QCD background shape, a smooth functional form

$$f(x) = p_1(1-x)^{p_2} x^{p_3+p_4 \ln x}, \quad (4)$$

where $x \equiv m_{jj}/\sqrt{s}$ and the p_i are fit parameters, is fitted to the dijet mass spectrum. Although not inspired by a theory, this functional form has been empirically shown to model the steeply falling QCD dijet mass spectrum [3, 5, 7]. Figure 2 shows the resulting mass spectrum and fitted background, indicating that the observed spectrum is consistent with a rapidly falling, smooth distribution. The bin widths have been chosen to be consistent with the dijet mass resolution,

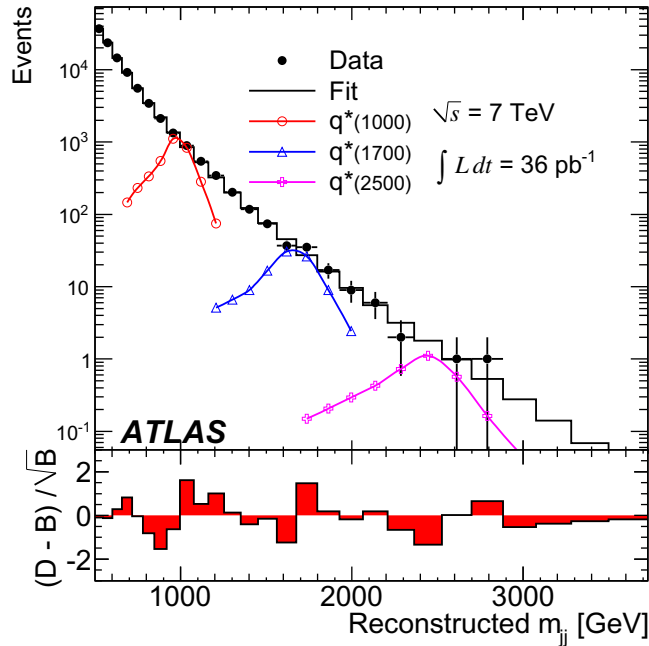


Figure 2. The observed (D) dijet mass distribution (filled points) fitted using a binned QCD background (B) distribution described by equation (4) (histogram). The predicted q^* signals normalized to 36 pb^{-1} for excited-quark masses of 1000, 1700 and 2500 GeV are overlaid. The bin-by-bin significance of the data-background difference is shown in the lower panel.

increasing from ~ 50 to ~ 200 GeV for dijet masses from 600 to 3500 GeV, respectively. The p -value of the fit to the data, calculated using the chi-squared test determined from pseudo-experiments as a goodness-of-fit statistic, is 0.88. Although this p -value suggests that there is no significant overall disagreement, we use a more sensitive statistical test, the BUMP HUNTER algorithm [43, 44], to establish the presence or absence of a resonance.

In its implementation in this analysis, the BUMP HUNTER algorithm searches for the signal window with the most significant excess of events above the background, requiring insignificant discrepancy (Poisson counting p -value $> 10^{-3}$) in both the adjacent sidebands. Starting with a two-bin window, the algorithm increases the signal window and shifts its location until all possible bin ranges, up to half the mass range spanned by the data, have been tested. The most significant departure from the smooth spectrum, defined by the set of bins that have the smallest probability of arising from a background fluctuation assuming Poisson statistics, is therefore identified. The algorithm accounts for the ‘trials factor’ to assess the significance (i.e., p -value) of its finding. It does this by performing a series of pseudo-experiments to determine the probability that random fluctuations in the background-only hypothesis would create an excess as significant as the observed one anywhere in the spectrum. The background to which the data are compared is obtained from the aforementioned fit, excluding the region with the biggest local excess of data in cases where the χ^2 test yields a p -value less than 0.01. Although this is not the case for the actual data, it can happen in some of the pseudo-experiments that are used to determine the p -value. The reason for this exclusion is to prevent potential new physics signal from biasing the background.

The most significant discrepancy identified by the BUMP HUNTER algorithm is a three-bin excess in the dijet mass interval 995–1253 GeV. The p -value, of observing an excess at least as large as this assuming a background-only hypothesis, is 0.39. We therefore conclude that there is no evidence for a resonance signal in the m_{jj} spectrum and proceed to set limits on various models.

5.2. Exclusion limits using the dijet mass

We set Bayesian credibility intervals by defining a posterior probability density from the likelihood function for the observed mass spectrum, obtained by a fit to the background functional form and a signal shape derived from MC calculations. A prior constant in the possible signal strength is assumed. The posterior probability is then integrated to determine the 95% credibility level (CL) for a given range of models, usually parameterized by the mass of the resonance. A Bayesian approach is employed for setting limits using the dijet mass distribution as it simplifies the treatment of systematic uncertainties.

The systematic uncertainties affecting this analysis arise from instrumental effects, such as the JES and resolution (JER) uncertainties, the uncertainty on the integrated luminosity and the uncertainties arising from the background parameterization. Extensive studies of the performance of the detector using both data and MC modelling have resulted in a JES uncertainty ranging from 3.2 to 5.7% in the current data sample [15]. The systematic uncertainty in the integrated luminosity is 11% [45]. The uncertainties in the background parameterization are taken from the fit results discussed earlier and range from 3% at 600 GeV to $\sim 40\%$ at 3500 GeV. These uncertainties are incorporated into the analysis by varying all the sources according to Gaussian probability distributions and convolving these with the Bayesian posterior probability distribution. Credibility intervals are then calculated numerically from the resulting convolutions.

Uncertainties in the signal models come primarily from our choice of PDFs and the tune for the PYTHIA MC, which provides the best match of observed data with the predictions with that choice of PDF. Our default choice of PDFs for the dijet mass analysis is MRST2007LO* [20] with the MC09 tune [19]. Limits are quoted also using CTEQ6L1 and CTEQ5L PDF sets, which provide an alternative PDF parameterization and allow comparisons with previous results [3], respectively. For the q^* limit analysis, we also vary the renormalization and factorization scales in the PYTHIA calculation by factors of one-half and two and find that the observed limit varies by ~ 0.1 TeV.

5.3. Limits on excited quark production

The particular signal hypothesis used to set limits on excited quarks (q^*) has been implemented using the PYTHIA MC generator, with fixed parameters to specify the excited quark mass, m_{q^*} , and its decay modes, as discussed in section 4. Each choice of mass constitutes a specific signal template, and a high-statistics set of MC events was created and fully simulated for each choice of m_{q^*} . The acceptance, \mathcal{A} , of our selection requirements ranges from 49 to 58% for m_{q^*} from 600 to 3000 GeV, respectively. The loss of acceptance comes mainly from the pseudorapidity requirements, which ensure that the candidate events have a high signal-to-background ratio.

In figure 3 the resulting 95% CL limits on $\sigma \cdot \mathcal{A}$ for excited quark production are shown as a function of the excited quark mass, where σ is the cross section for production of resonance

Table 1. The 95% CL lower limits on the allowed q^* mass obtained using different tunes and PDF sets. The MC09' tune is identical to MC09 except for the PYTHIA parameter $\text{PARP}(82) = 2.1$ and the use of the CTEQ6L1 PDF set.

MC tune	PDF set	Observed limit (TeV)		Expected limit (TeV)	
		Stat. \oplus syst.	Stat. only	Stat. \oplus syst.	Stat. only
MC09 [19]	MRST2007LO* [20]	2.15	2.27	2.07	2.12
MC09'	CTEQ6L1 [46]	2.06	2.19	2.01	2.07
Perugia0 [47]	CTEQ5L [48]	2.14	2.26	2.06	2.12

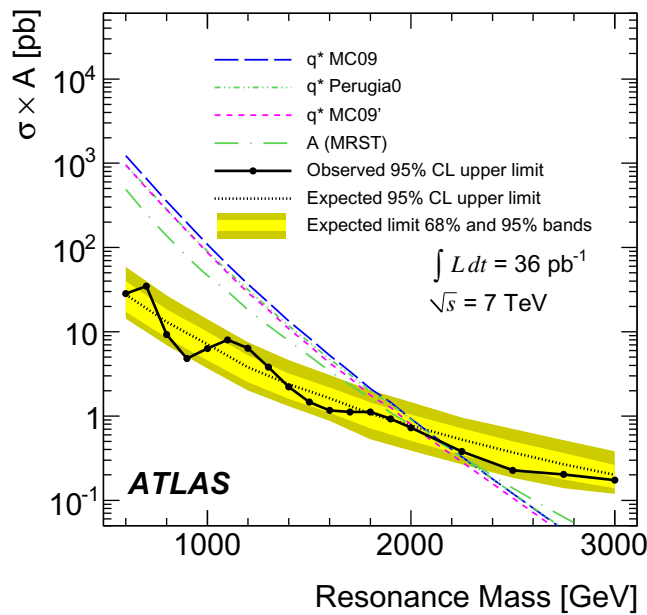


Figure 3. The 95% CL upper limits on the cross section times acceptance for a resonance decaying to dijets taking into account both statistical and systematic uncertainties (points and solid line) compared to an axigluon model and to a q^* model with three alternative MC tunes. We also show the expected limit (dotted line) and the 68 and 95% contours of the expected limit (bands).

and \mathcal{A} is the acceptance for the dijet final state. The expected limit is also shown, based on the statistics of the sample and assuming a background-only hypothesis. We see that the observed and expected limits are in reasonable agreement with each other, strengthening our earlier conclusion that there is no evidence of a signal above the smooth background. Comparing the observed limit with the predicted q^* cross section times acceptance, we exclude at 95% CL q^* masses in the interval $0.60 < m_{q^*} < 2.15$ TeV. The expected limit excludes $m_{q^*} < 2.07$ TeV.

The sensitivity of the resulting limit to the choice of PDFs was modest, as shown in table 1 where the observed and expected mass limits are compared for several other models. In all cases, the mass limits vary by less than 0.1 TeV. The inclusion of systematic uncertainties results in modest reductions in the limit, illustrating that the limit setting is dominated by statistical uncertainties.

Table 2. The 95% CL lower limits on the allowed quantum gravity scale for various numbers of extra dimensions.

Number of extra dimensions	Observed M_D limit (TeV)		Expected M_D limit (TeV)	
	Stat. \oplus Syst.	Stat. only	Stat. \oplus Syst.	Stat. only
2	3.20	3.22	3.18	3.20
3	3.38	3.39	3.35	3.37
4	3.51	3.52	3.48	3.50
5	3.60	3.61	3.58	3.59
6	3.67	3.68	3.64	3.66
7	3.73	3.74	3.71	3.72

5.4. Limits on axigluon production

We set limits on axigluon production using the same procedure followed for the q^* analysis, creating templates for the signal using the axigluon model described in section 4 and full detector simulation. There are large non-resonant contributions to the cross section at low dijet mass, so we require at the parton-level that the axigluon invariant mass be between 0.7 and 1.3 times the nominal mass of the resonance. Having made this requirement, we note that the axigluon and q^* signal templates result in very similar limits. So for convenience we use the q^* templates in setting cross section limits on axigluon production.

The resulting limits are shown in figure 3. Using the MRST2007LO* PDFs, we exclude at 95% CL axigluon masses in the interval $0.60 < m < 2.10$ TeV. The expected limit is $m < 2.01$ TeV. If only statistical uncertainties are included, the limit rises by ~ 0.2 TeV, indicating that the systematic uncertainties are not dominant.

5.5. Limits on quantum black hole (QBH) production

We search for the production of QBHs as these are expected to produce low multiplicity decays with a significant contribution to dijet final states. Several scenarios are examined, with quantum gravity scales M_D ranging from 0.75 TeV to 4.0 TeV and with the number of extra dimensions, n , ranging from two to seven. The fully simulated MC events are used to create templates similar to the q^* analysis. These QBH models produce threshold effects in m_{jj} with long tails to higher m_{jj} that compete with the QCD background. However, the cross section is very large just above the threshold and so it is possible to extract limits given the resulting resonance-like signal shape.

The resulting limits are illustrated in figure 4, showing the observed and expected limits, as well as the predictions for QBH production assuming two, four and six extra dimensions. The observed lower limits on the quantum gravity scale, M_D , with and without systematic uncertainty, and the expected limit with and without systematic uncertainty, at 95% CL are summarized in table 2. Using CTEQ6.6 PDFs, we exclude at 95% CL quantum gravity scales in the interval $0.75 < M_D < 3.67$ TeV for the low-multiplicity QBHs with six extra dimensions. The expected limit is $M_D < 3.64$ TeV.

5.6. Limits on Randall–Sundrum (RS) graviton production

We search for the production of RS gravitons by creating dijet mass templates using the MC calculation described in section 4. In this case, the sensitivity of the search is reduced by the

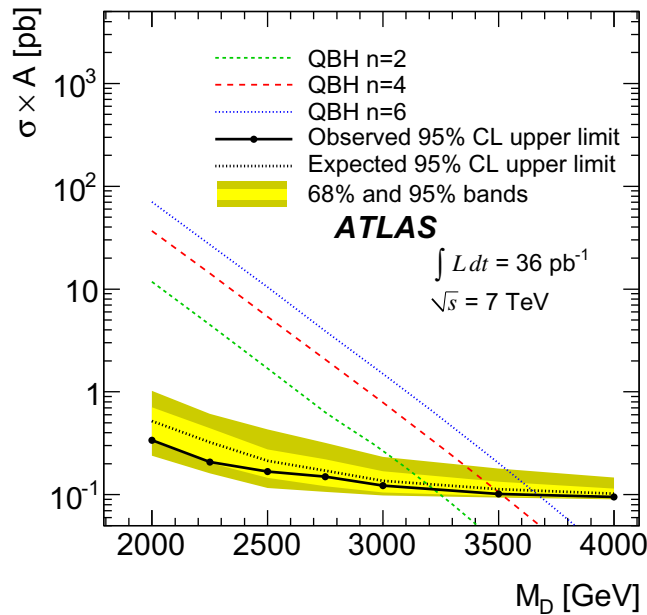


Figure 4. The 95% CL upper limits on the cross section \times acceptance versus the quantum gravity mass scale M_D for a QBH model, taking into account both statistical and systematic uncertainties. The cross section \times acceptance for QBH models with two, four and six extra dimensions is shown. The 68 and 95% CL contours of the expected limit are shown as the band.

lower production cross section, and by our kinematic criteria that strongly select for final states that have either high-energy hadronic jets or EM showers.

The limits obtained for this hypothesis are illustrated in figure 5, showing the observed and expected limits, as well as the predictions for RS graviton production. It is not possible to exclude any RS graviton mass hypothesis, given the small expected signal rates and the relatively large QCD backgrounds. A limit on RS graviton models could be established with increased statistics, although more sophisticated strategies to improve signal-to-background may be necessary.

5.7. Simplified Gaussian model limits

We have used these data to set limits in a more model-independent way by employing as our signal template a Gaussian profile with means ranging from 600 GeV to 4000 GeV and with the width, σ , varying from 3 to 15% of the mean.

Systematic uncertainties are treated in the same manner as described previously, using pseudo-experiments to marginalize the posterior probabilities that depend on parameters that suffer from systematic uncertainty. However, given that the decay of the dijet final state has not been modelled, assuming only that the resulting dijet width is Gaussian in shape, we adjusted the treatment of the JES by modelling it as an uncertainty in the central value of the Gaussian signal.

The 95% CL limits are shown in table 3, expressed in terms of the number of events observed after all event selection criteria have been applied. We stress that these event limits

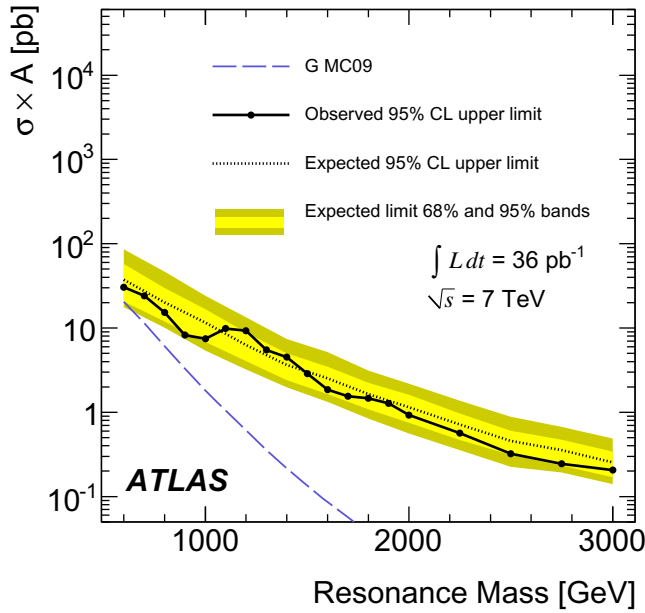


Figure 5. The 95% CL upper limits on the cross section \times acceptance for an RS graviton, taking into account both statistical and systematic uncertainties. The 68 and 95% CL contours of the expected limit are shown as the band.

are determined by assuming a Gaussian signal shape. Their variation as a function of mass and width reflects the statistical fluctuations of data in the binned m_{jj} distribution used to set them.

These limits can be employed by computing for a given model the acceptance \mathcal{A} using a standard MC calculation. The jet p_T and η requirements should first be applied to determine the expected signal shape in m_{jj} . Since a Gaussian signal shape has been assumed in determining the limits, we recommend removing any long tails in m_{jj} (a $\pm 20\%$ mass window is recommended). The fraction of MC events surviving these requirements is an estimate of the acceptance, and can be used to calculate the expected event yield given a cross section for the process and assuming a sample size of 36 pb^{-1} . This event yield can then be compared with the limit in table 3, matching the expected signal mean and width to the appropriate entry in the table.

6. Angular distribution analyses

For all angular distribution analyses, the common event selection criteria described in section 3 are applied, including the transverse momentum requirements on the two leading jets: $p_T^{j_1} > 60 \text{ GeV}$ and $p_T^{j_2} > 30 \text{ GeV}$. Additionally, χ distributions are accumulated only for events that satisfy $|y_B| < 1.10$ and $|y^*| < 1.70$. The $|y^*|$ criterion determines the maximum χ of 30 for this analysis. These two criteria limit the rapidity range of both jets to $|y_{1,2}| < 2.8$ and define a region within the space of accessible y_1 and y_2 with full and uniform acceptance in χ at $m_{jj} > 500 \text{ GeV}$. These kinematic cuts have been optimized by MC studies of QCD and new physics signal samples to ensure high acceptance for all dijet masses.

Detector resolution effects smear the χ distributions, causing events to migrate between neighbouring bins. This effect is reduced by choosing the χ bins to match the natural segmentation of the calorimeter, making them intervals of constant Δy for these high- p_T dijet

Table 3. The 95% CL upper limits on the number of observed signal events for Gaussian reconstructed m_{jj} distributions. The effects of systematic uncertainties due to the luminosity, the background fit and the JES have been included. We present the signal widths as σ/m .

Mean m (GeV)	σ/m				
	0.03	0.05	0.07	0.10	0.15
600	434	638	849	1300	1990
700	409	530	789	1092	945
800	173	194	198	218	231
900	88	103	123	162	311
1000	147	179	210	278	391
1100	143	169	204	263	342
1200	91	120	168	223	262
1300	65	80	101	120	122
1400	35	42	50	57	66
1500	24	27	32	40	60
1600	21	25	29	36	49
1700	26	27	28	38	43
1800	25	26	30	32	34
1900	22	22	25	25	26
2000	13	16	19	19	17
2100	10	12	14	16	17
2200	8.4	9.4	11	10	11
2300	6.8	7.3	7.4	8.3	9.0
2400	4.9	5.2	6.1	6.6	8.0
2500	4.6	4.9	5.4	6.4	6.9
2600	4.9	5.0	5.3	6.0	6.6
2700	5.1	5.0	5.0	5.2	5.7
2800	5.0	5.0	4.9	5.0	5.2
2900	4.6	4.5	4.7	4.6	4.8
3000	4.1	4.2	4.3	4.5	4.7
3200	3.2	3.5	3.6	3.8	4.1
3400	3.1	3.1	3.2	3.5	3.7
3600	3.1	3.1	3.1	3.3	3.6
3800	3.1	3.1	3.1	3.2	3.3
4000	3.1	3.1	3.1	3.1	3.3

events. The F_χ and $F_\chi(m_{jj})$ variables are even less sensitive to migration effects, given that they depend on separation of the data sample into only two χ intervals.

6.1. Systematic and statistical uncertainties

Dijet angular distribution analyses have a reduced sensitivity to the JES and JER uncertainties compared to other dijet measurements because data and theoretical distributions are normalized to unit area for each mass bin in all cases. Nevertheless, the JES still represents the dominant systematic uncertainty in the current studies.

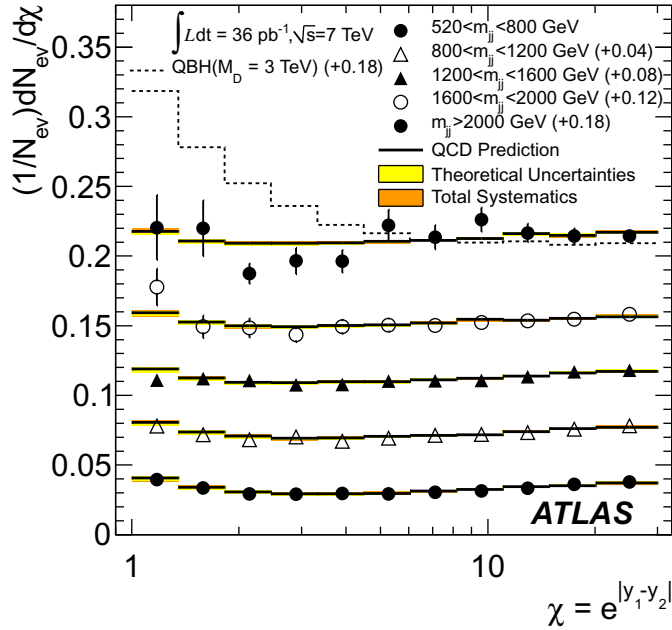


Figure 6. The χ distributions for $520 < m_{jj} < 800$ GeV, $800 < m_{jj} < 1200$ GeV, $1200 < m_{jj} < 1600$ GeV, $1600 < m_{jj} < 2000$ GeV and $m_{jj} > 2000$ GeV. Shown are the QCD predictions with systematic uncertainties (narrow bands), and data points with statistical uncertainties. The dashed line is the prediction for a QBH signal for $M_D = 3$ TeV and $n = 6$ in the highest mass bin. The distributions and QCD predictions have been offset by the amount shown in the legend to aid in visually comparing the shapes in each mass bin.

As described in a previous publication [6], our dijet angular analyses use pseudo-experiments to convolve statistical, systematic and theoretical uncertainties. The primary sources of theoretical uncertainty are NLO QCD renormalization (μ_R) and factorization scales (μ_F) and PDF uncertainties. The former are varied by a factor of two, independently, while the PDF errors are sampled from a Gaussian distribution determined using CTEQ6.6 (NLO) PDF error sets. The resulting bin-wise uncertainties for normalized χ distributions are typically up to 3% for the combined NLO QCD scales and 1% for the PDF uncertainties. These convolved experimental and theoretical uncertainties are calculated for all MC angular distributions (both QCD and new physics samples). These statistical ensembles are used for estimating p -values when comparing QCD predictions to data and for parameter determination when setting limits.

6.2. Observed χ and $F_\chi(m_{jj})$ distributions

The analysis method used in the first ATLAS publication on this topic [6] is revisited here for the full 2010 data sample. The χ distributions are shown in figure 6 for several relatively large m_{jj} bins, defined by the bin boundaries of 520, 800, 1200, 1600 and 2000 GeV. There are 71 402 events in the sample, ranging from 42 116 events in the lowest mass bin to 212 events with $m_{jj} > 2000$ GeV. These bins were chosen to ensure sufficient statistics in each mass bin. This is most critical for the highest mass bin—the focal point for new physics searches. The χ distributions are compared in the figure to the predictions from QCD MC models and the

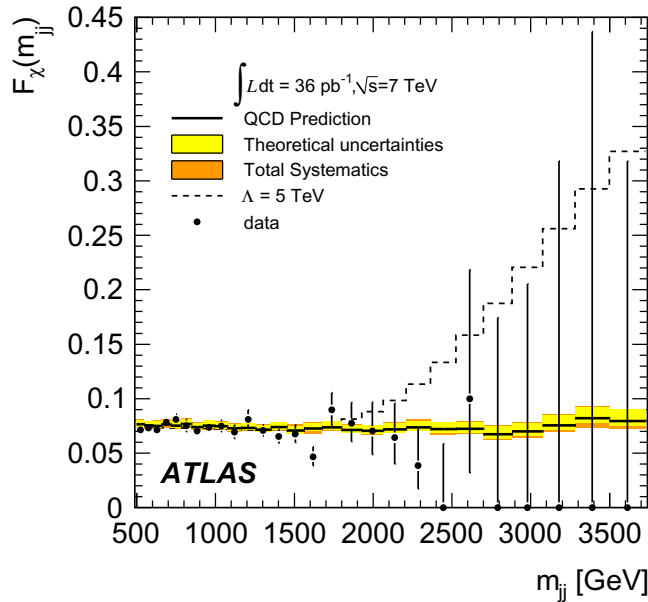


Figure 7. The $F_\chi(m_{jj})$ function versus m_{jj} . We show the QCD prediction with systematic uncertainties (band), and data points (black points) with statistical uncertainties. The expected signal from QCD plus a quark contact interaction with $\Lambda = 5.0$ TeV is also shown.

signal that would be seen in one particular new physics model, a QBH scenario with a quantum gravity mass scale of 3 TeV and six extra dimensions.

The data appear to be consistent with the QCD predictions, which include systematic uncertainties. To verify this, a binned likelihood is calculated for each distribution assuming that the sample consists only of QCD dijet production. The expected distribution of this likelihood is then calculated using pseudo-experiments drawn from the QCD MC sample and convolved with the systematic uncertainties as discussed above. The p -values for the observed likelihood values, from the lowest to highest mass bins, are 0.44, 0.33, 0.64, 0.89 and 0.44, respectively, confirming that the SM QCD hypothesis is consistent with the data.

We compute the $F_\chi(m_{jj})$ observable, introduced in section 2, using the same mass binning employed in the dijet resonance searches. The observed $F_\chi(m_{jj})$ data are shown in figure 7 and are compared to the QCD predictions, which include systematic uncertainties. We also show the expected behaviour of $F_\chi(m_{jj})$ if a contact interaction with the compositeness scale $\Lambda = 5.0$ TeV were present. Statistical analyses using $F_\chi(m_{jj})$ use mass bins starting at 1253 GeV to be most sensitive to the high dijet mass region. Assuming only QCD processes and including systematic uncertainties, the p -value for the observed binned likelihood is 0.28, indicating that these data are consistent with QCD predictions.

In the absence of any evidence for signals associated with new physics phenomena, these distributions are used to set 95% CL exclusion limits on a number of new physics hypotheses.

6.3. Exclusion limits from likelihood ratios

Most of the dijet angular distribution analyses described below use likelihood ratios to compare different hypotheses and parameter estimation. Confidence level limits are set using the

frequentist $\text{CL}_{\text{s+b}}$ approach [49]. As an example, for the $F_\chi(m_{jj})$ distributions the variable Q is defined as follows:

$$Q = -2[\ln L(F_\chi(m_{jj})|H0) - \ln L(F_\chi(m_{jj})|H1)], \quad (5)$$

where $H0$ is the null hypothesis (QCD only), $H1$ is a specific hypothesis for new physics with fixed parameters and $L(F_\chi(m_{jj})|H)$ is the binned likelihood for the $F_\chi(m_{jj})$ distribution assuming H as the hypothesis. Pseudo-experiments are used to determine the expected distribution for Q for specific hypotheses. The new physics hypothesis is then varied to calculate a Neyman confidence level.

6.4. Limits on quark contact interactions

The $F_\chi(m_{jj})$ variable is used for the first time in this paper to set limits on quark contact interactions (CI), as described in section 4. MC samples of QCD production modified by a CI are created for values of Λ ranging from 0.50 to 8.0 TeV.

For the pure QCD sample (corresponding to $\Lambda = \infty$), the $F_\chi(m_{jj})$ distribution is fitted to a second order polynomial. For MC samples with finite Λ , the distributions are fitted, as a function of m_{jj} , to the second order polynomial plus a Fermi function, which is a good representation of the onset curve for CIs. QCD K -factors from section 4 are applied to the QCD-only component of the spectra before calculating $F_\chi(m_{jj})$. This is done through an approximation that neglects possible NLO corrections in the interference term between the QCD matrix element and the CI term. The issue of NLO corrections to contact terms has been independently identified elsewhere [50].

The $F_\chi(m_{jj})$ event sample is fitted in each m_{jj} bin of the distribution as a function of $1/\Lambda^2$, creating a predicted $F_\chi(m_{jj})$ surface as a function of m_{jj} and Λ . This surface enables integration in m_{jj} versus Λ for continuous values of Λ . Using this surface, the 95% CL limit on Λ is determined using the log-likelihood ratio defined in equation (5). The resulting 95% CL quantile is shown in figure 8.

Figure 8 also shows the expected value of Q for various choices of Λ as well as the expected 95% CL limit and its 68% contour interval.

The observed exclusion limit is found from the point where the 95% quantile (dotted line) crosses the median value of the distribution of Q values for the QCD prediction (dashed line). This occurs at $\Lambda = 9.5$ TeV. The expected limit is $\Lambda = 5.7$ TeV. The observed result is significantly above the expected limit because the data have fewer centrally produced, high mass dijet events than expected from QCD alone, as can be seen in figure 7 where the observed values of $F_\chi(m_{jj})$ fall below the QCD prediction for dijet masses around 1.6 TeV and above 2.2 TeV. These data are statistically compatible with QCD, as evidenced by the p -value of the binned likelihood. The expected probability that a limit at least as strong as this would be observed is $\sim 8\%$.

As a cross-check, a Bayesian analysis of $F_\chi(m_{jj})$ has been performed, assuming a prior that is constant in $1/\Lambda^2$. This analysis sets a 95% credibility level of $\Lambda > 6.7$ TeV. The expected limit from this Bayesian analysis is 5.7 TeV, comparable to the $\text{CL}_{\text{s+b}}$ expected limit. While the observed limit from $\text{CL}_{\text{s+b}}$ analysis is significantly higher than the Bayesian results, we have no basis on which to exclude the $\text{CL}_{\text{s+b}}$ result *a posteriori*.

As an additional cross-check, the earlier F_χ analysis of the $dN/d\chi$ distributions, coarsely binned in m_{jj} [6], has been repeated. With the larger data sample and higher threshold on the

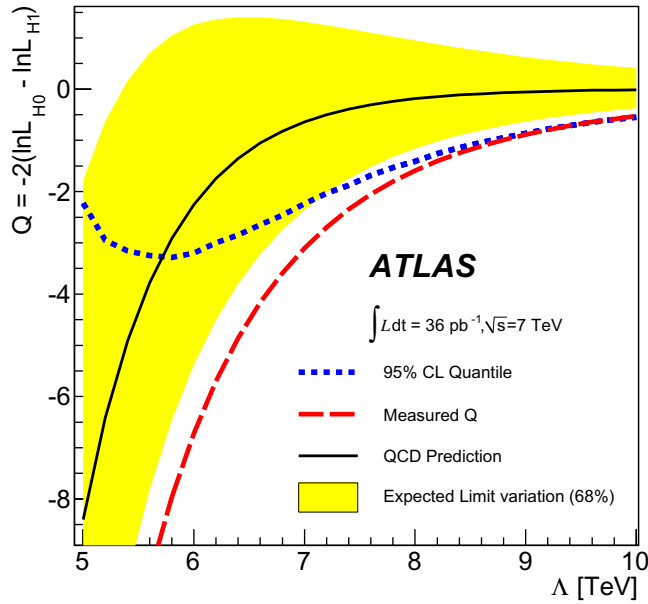


Figure 8. The log-likelihood ratio defined by the $F_\chi(m_{jj})$ distribution versus the strength of the contact interaction, Λ . The contact interaction limit is set by comparing the measured log-likelihood ratio to that expected for a given value of Λ .

highest m_{jj} bin (2 TeV), the observed and expected limits are $\Lambda > 6.8$ TeV and $\Lambda > 5.2$ TeV, respectively. As anticipated, these limits are not as strong as those arising from the $F_\chi(m_{jj})$ analysis because of the coarser m_{jj} binning.

Finally, an analysis was performed to see whether a more sensitive measure could be created by setting limits based on all 11 bins of the highest mass ($m_{jj} > 2$ TeV) χ distribution, instead of the two intervals used in the F_χ analysis. In this method, for each bin the same interpolating function used in the $F_\chi(m_{jj})$ analysis is fitted to the bin contents resulting from all QCD + CI MC samples, yielding the CI onset curve. Limits are set using the same log-likelihood ratio and pseudo-experiment methods employed in the $F_\chi(m_{jj})$ analysis. The observed 95% CL limit is $\Lambda > 6.6$ TeV. For the current data sample, the expected limit is 5.4 TeV. Since the expected limit exceeds that from the F_χ analysis, this method shows promise for future analyses.

6.5. Limits on excited quark production

The $F_\chi(m_{jj})$ distributions are also used to set limits on excited quark production. As described earlier, the q^* model depends only on the single parameter, m_{q^*} . Twelve simulated q^* mass (m_{q^*}) samples in the range of 1.5–5.0 TeV are used for the analysis. Based on the assumption that interference of QCD with excited quark resonances is negligible, q^* MC samples are scaled by their cross sections and added to the NLO QCD sample (which has been corrected using bin-wise K -factors). By analogy with the CI analysis above, a likelihood is constructed by comparing the expected and observed $F_\chi(m_{jj})$ distributions for each value of m_{q^*} . We then form a likelihood ratio with respect to the QCD-only hypothesis and use this to set confidence intervals on the production of a q^* .

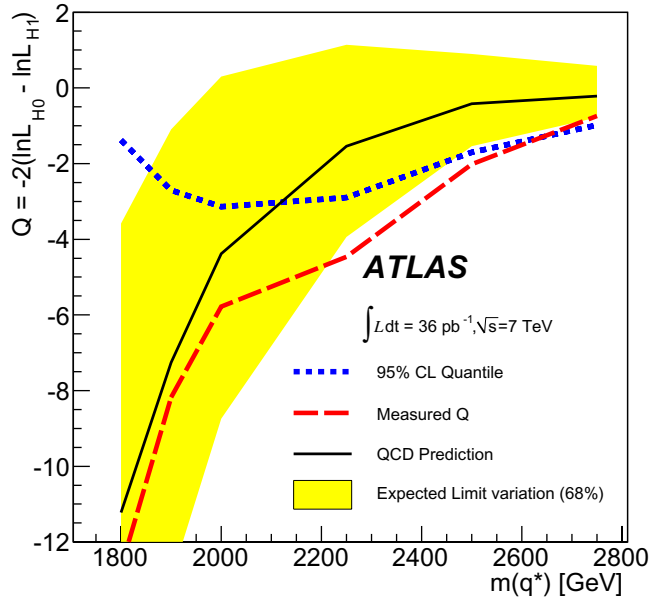


Figure 9. The 95% CL limits on the excited quark model using the logarithm of the likelihood ratios obtained from the $F_{\chi}(m_{jj})$ distribution. The expected 68% interval for the expected limits are shown by the band.

Figure 9 illustrates the limit setting procedure for the q^* model. The observed exclusion limit is found from the point where the 95% quantile (dotted line) crosses the measured value of Q (dashed line). This occurs for $m_{q^*} = 2.64$ TeV. The expected limit, determined from the point where the QCD prediction (solid line) crosses the 95% quantile, is 2.12 TeV. The observed limit falls near the 68% ($\pm 1\sigma$) interval of the expected limit. The difference between observed and expected limits arises from the lower observed $F_{\chi}(m_{jj})$ values at dijet masses above 2.2 TeV.

This result can be compared to the limits obtained from the dijet resonance analysis, which sets observed exclusion limits on q^* masses of 2.15 TeV.

6.6. Limits on new physics for additive signals

For new physics signals that do not interfere significantly with QCD, limit setting may be done in a more model-independent way. MC signal samples are simulated independently from QCD samples and, for a given choice of new physics model parameters, the two samples are added to create a combined MC sample for comparison with data. This is implemented by introducing a variable θ_{np} defined as

$$\theta_{np} = \frac{\sigma_{np} \times \mathcal{A}_{np}}{\sigma_{\text{QCD}} \times \mathcal{A}_{\text{QCD}}}, \quad (6)$$

where σ and \mathcal{A} are the cross section and acceptance for the given process, and ‘ np ’ refers to the new physics process. This variable represents the contribution of signal events in terms of cross section times acceptance relative to the QCD background. The acceptance factors are determined by MC calculations.

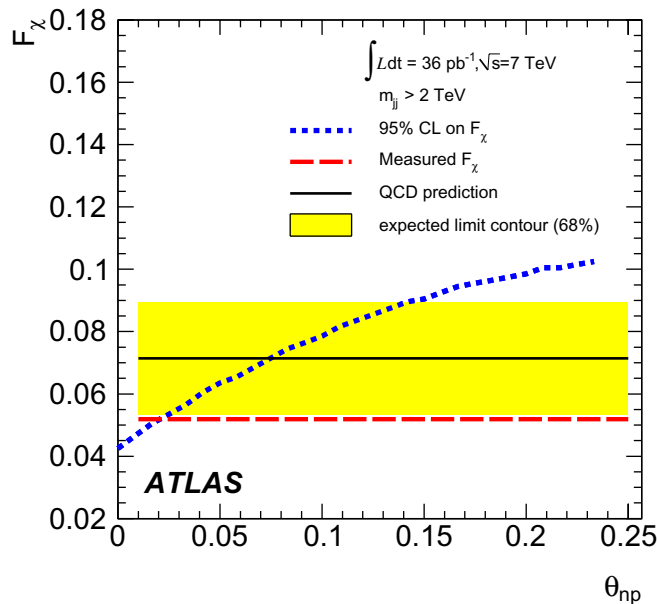


Figure 10. The 95% CL upper limits in the F_χ – θ_{np} plane for QBH production for $n = 6$ extra dimensions.

6.7. Limits on QBH production

The model of QBH production [39, 40], introduced in section 4 and used to set limits on these phenomena in the dijet resonance analysis, is again employed here to search for QBH production using the dijet angular distributions. The θ_{np} -parameter limit-setting method, sensitive to $\sigma_{\text{QBH}} \times \mathcal{A}_{\text{QBH}}$, is used in this analysis since the QBH production model does not include interference with QCD.

MC samples are created corresponding to discrete values of the QBH quantum gravity mass scale M_D ranging from 2.0 to 4.0 TeV and for two to seven extra dimensions (n), and are used to determine the acceptance \mathcal{A}_{QBH} . The acceptance is found to vary from 58 to 89% as M_D is varied from 2.0 to 4.0 TeV, for the case of six extra dimensions. These studies have shown that the signal acceptance for the model considered here varies only slightly with the model parameter n . Thus, \mathcal{A}_{QBH} determined from a full simulation of the sample with $n = 6$ is applied to a limit analysis for other choices of n , which have different cross sections.

The MC events with dijet masses greater than 2.0 TeV are binned in χ with the same bin boundaries as those used in figure 6. Pseudo-experiments are used to incorporate the JES uncertainty into the predicted χ distributions. In each χ bin, a linear fit is made for $dN/d\chi$ versus θ_{np} , creating a family of lines that define a $dN/d\chi$ surface in θ_{np} versus χ . Scale and PDF uncertainties, and the uncertainty in the JES correlation between the two jets, are incorporated into this surface using pseudo-experiments, and a value of F_χ is calculated from each distribution. The expected distributions of F_χ values are obtained for a range of QBH hypotheses and QCD processes alone. Additional pseudo-experiments are used to model the finite statistics of the high- m_{jj} event sample. The 95% CL exclusion limit on F_χ , as a function of θ_{np} , is derived from the resulting likelihood distributions of F_χ .

Figure 10 illustrates the θ_{np} parameter limit-setting procedure for the case $n = 6$. The observed exclusion limit is found from the point where the 95% CL contour (dotted line) crosses

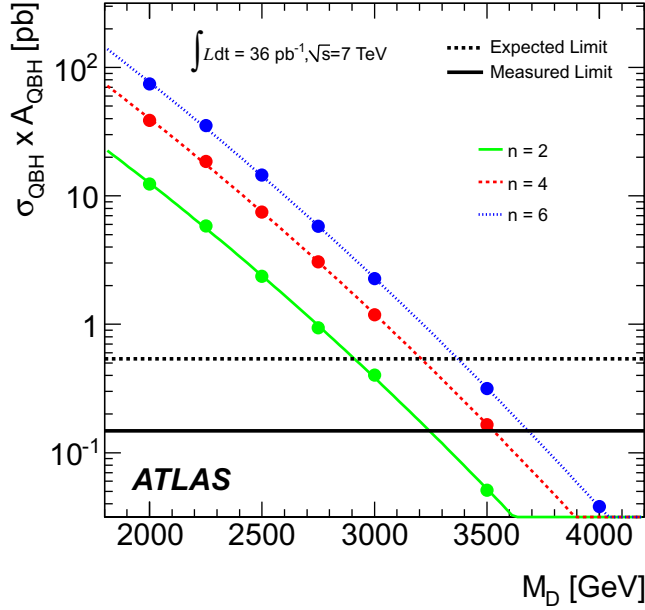


Figure 11. The cross section \times acceptance for QBHs as a function of M_D for two, four and six extra dimensions. The measured and expected limits are shown in the solid and dashed lines.

the measured value of $F_\chi = 0.052$ (dashed line), which occurs at $\theta_{np} = 0.020$. The expected limit, determined from the point where the QCD prediction, 0.071 (solid line), crosses the 95% CL contour, is at 0.075. The observed limit falls just outside the 68% ($\pm 1\sigma$) interval of the expected limit. These limits on θ_{np} are translated into limits on $\sigma \times \mathcal{A}$ using the QCD cross section and the acceptance for fully simulated dijets, $\sigma_{\text{QCD}} \times \mathcal{A}_{\text{QCD}} = 7.21$ pb, resulting in an observed 95% CL upper limit $\sigma_{\text{QBH}} \times \mathcal{A}_{\text{QBH}} < 0.15$ pb.

Figure 11 shows the $\sigma_{\text{QBH}} \times \mathcal{A}_{\text{QBH}}$ versus M_D curves for two, four and six extra dimensions. The measured and expected limits for $\sigma_{\text{QBH}} \times \mathcal{A}_{\text{QBH}}$ are plotted as horizontal lines. The crossing points of these lines with the n versus M_D curve yield expected and observed exclusion limits for the QBH model studied here. The 95% CL lower limit on the quantum gravity mass scale is 3.69 TeV for six extra dimensions. The expected limit is 3.37 TeV. The limits for all extra dimensions studied here, $n = 2-7$, are listed in table 4.

The limit for $\sigma_{\text{QBH}} \times \mathcal{A}_{\text{QBH}}$ may also be applied to any new physics model that satisfies the following criteria: (1) the F_χ of np signal-only event samples should be roughly independent of m_{jj} , as is the case for q^* , QBH and CIs; and (2) this F_χ should be close to the value of F_χ for the current QBH study [0.58]. It is not necessary that the m_{jj} spectrum be similar or that the QCD + np sample have the same F_χ .

It should also be noted that the results from this θ_{np} parameter analysis are in agreement with the expected and observed limits obtained for the same QBH model in the dijet resonance analysis. These two analyses are focusing on complementary variables in the two-dimensional space of m_{jj} and χ yet arrive at similar limits.

A cross-check of these results is made by extracting a QBH limit using the $F_\chi(m_{jj})$ distribution for the case of six extra dimensions. Signal and background samples are created by combining the QBH signals for various M_D 's with the QCD background sample corrected

Table 4. The 95% CL exclusion limits on M_D for various choices of extra dimensions for the QBH model determined by the θ_{np} parameter analysis for at $m_{jj} > 2.0$ TeV.

n extra dimensions	Expected limit (TeV)	Observed limit (TeV)
2	2.91	3.26
3	3.08	3.41
4	3.20	3.53
5	3.29	3.62
6	3.37	3.69
7	3.43	3.75

by K -factors. The $F_\chi(m_{jj})$ distribution is then fitted in each m_{jj} bin as a function of $1/M_D^2$ using the same interpolating function employed in $F_\chi(m_{jj})$ CI analysis. The likelihood ratio construction and limit setting procedures used in the CI analysis are also applied in this study, resulting in observed and expected 95% CL limits for M_D of 3.78 and 3.49 TeV, respectively. A further cross-check is performed using the 11-bin χ analysis to set limits on a QBH for the case of six extra dimensions. This study yields an observed 95% CL limit of $M_D > 3.49$ TeV and an expected limit of $M_D > 3.36$ TeV.

The expected and observed limits resulting from these four studies are summarized with the results of other analyses in table 5. The strongest expected limits on QBH production come from the dijet resonance analysis, but the angular analyses are in close agreement, yielding limits within 0.3 TeV of each other for the QBH hypothesis under study.

7. Conclusion

Dijet mass and angular distributions have been measured by the ATLAS experiment over a large angular range and spanning dijet masses up to ≈ 3.5 TeV using 36 pb^{-1} of 7 TeV pp collision data. The angular distributions are in good agreement with QCD predictions and we find no evidence for new phenomena. Our analysis, employing both the dijet mass and the dijet angular distributions, places the most stringent limits on contact interactions, resonances and threshold phenomena to date.

In table 5, the constraints on specific models of new physics that would contribute to dijet final states are summarized.

We quote as the primary results the limits using the technique with the most stringent expected limit. Therefore, we exclude at 95% CL excited quarks with masses in the interval $0.60 < m_{q^*} < 2.64$ TeV, axigluons with masses between 0.60 TeV and 2.10 TeV, and QBHs with $0.75 < M_D < 3.67$ TeV assuming six extra dimensions.

We also exclude at 95% CL quark contact interactions with a scale $\Lambda < 9.5$ TeV. As noted earlier, the observed limit is significantly above the expected limit of 5.7 TeV for this data sample, and above the limits from an alternative calculation using Bayesian statistics. However, we quote this result since the statistical approach is a standard procedure that was chosen *a priori*.

Table 5. The 95% CL lower limits on the masses and energy scales of the models examined in this study. We have included systematic uncertainties in the upper limits using the techniques described in the text. The result with the highest expected limit is shown in boldface and is our quoted result.

Model and analysis strategy	95% CL limits (TeV)	
	Expected	Observed
Excited quark q^*		
Resonance in m_{jj}	2.07	2.15
$F_\chi(m_{jj})$	2.12	2.64
QBH for $n = 6$		
Resonance in m_{jj}	3.64	3.67
$F_\chi(m_{jj})$	3.49	3.78
θ_{np} parameter for $m_{jj} > 2$ TeV	3.37	3.69
11-bin χ distribution for $m_{jj} > 2$ TeV	3.36	3.49
Axigluon		
Resonance in m_{jj}	2.01	2.10
Contact interaction Λ		
$F_\chi(m_{jj})$	5.7	9.5
F_χ for $m_{jj} > 2$ TeV	5.2	6.8
11-bin χ distribution for $m_{jj} > 2$ TeV	5.4	6.6

In a number of cases, searches for the same phenomenon have been performed using dijet mass distributions, dijet angular distributions or both. We are able to set comparable limits using these complementary techniques, while at the same time searching for evidence of narrow resonances, threshold effects and enhancements in angular distributions that depend on the dijet invariant mass.

This combined analysis is a sensitive probe into new physics that is expected to emerge at the TeV scale. With increased integrated luminosity and continued improvements to analysis techniques and models, we expect to increase the ATLAS discovery reach for new phenomena that affect dijet final states.

Acknowledgments

We thank CERN for the highly successful operation of the LHC and we also thank the support staff from our institutions without whom ATLAS could not have been operated efficiently. We acknowledge support from ANPCyT, Argentina; YerPhI, Armenia; ARC, Australia; BMWF, Austria; ANAS, Azerbaijan; SSTC, Belarus; CNPq and FAPESP, Brazil; NSERC, NRC and CFI, Canada; CERN; CONICYT, Chile; CAS, MOST and NSFC, China; COLCIENCIAS, Colombia; MSMT CR, MPO CR and VSC CR, Czech Republic; DNRF, DNSRC and Lundbeck Foundation, Denmark; ARTEMIS, European Union; IN2P3-CNRS, CEA-DSM/IRFU, France; GNAS, Georgia; BMBF, DFG, HGF, MPG and AvH Foundation, Germany; GSRT, Greece; ISF, MINERVA, GIF, DIP and Benoziyo Center, Israel; INFN, Italy; MEXT and JSPS, Japan; CNRST, Morocco; FOM and NWO, Netherlands; RCN, Norway; MNiSW, Poland; GRICES

and FCT, Portugal; MERYs (MECTS), Romania; MES of Russia and ROSATOM, Russian Federation; JINR; MSTD, Serbia; MSSR, Slovakia; ARRS and MVZT, Slovenia; DST/NRF, South Africa; MICINN, Spain; SRC and Wallenberg Foundation, Sweden; SER, SNSF and Cantons of Bern and Geneva, Switzerland; NSC, Taiwan; TAEK, Turkey; STFC, the Royal Society and Leverhulme Trust, UK; DOE and NSF, USA. The crucial computing support from all WLCG partners is also acknowledged, in particular from CERN and not only the ATLAS Tier-1 facilities at TRIUMF (Canada), NDGF (Denmark, Norway and Sweden), CC-IN2P3 (France), KIT/GridKA (Germany), INFN-CNAF (Italy), NL-T1 (Netherlands), PIC (Spain), ASGC (Taiwan), RAL (UK) and BNL (USA) but also the Tier-2 facilities worldwide.

The ATLAS Collaboration

G Aad⁴⁸, B Abbott¹¹¹, J Abdallah¹¹, A A Abdelalim⁴⁹, A Abdesselam¹¹⁸, O Abidinov¹⁰, B Abi¹¹², M Abolins⁸⁸, H Abramowicz¹⁵³, H Abreu¹¹⁵, E Acerbi^{89a,89b}, B S Acharya^{164a,164b}, D L Adams²⁴, T N Addy⁵⁶, J Adelman¹⁷⁵, M Aderholz⁹⁹, S Adomeit⁹⁸, P Adragna⁷⁵, T Adye¹²⁹, S Aefsky²², J A Aguilar-Saavedra^{124b,178}, M Aharrouche⁸¹, S P Ahlen²¹, F Ahles⁴⁸, A Ahmad¹⁴⁸, M Ahsan⁴⁰, G Aielli^{133a,133b}, T Akdogan^{18a}, T P A Åkesson⁷⁹, G Akimoto¹⁵⁵, A V Akimov⁹⁴, A Akiyama⁶⁷, M S Alam¹, M A Alam⁷⁶, S Albrand⁵⁵, M Aleksa²⁹, I N Aleksandrov⁶⁵, M Aleppo^{89a,89b}, F Alessandria^{89a}, C Alexa^{25a}, G Alexander¹⁵³, G Alexandre⁴⁹, T Alexopoulos⁹, M Alhroob²⁰, M Aliev¹⁵, G Alimonti^{89a}, J Alison¹²⁰, M Aliyev¹⁰, P P Allport⁷³, S E Allwood-Spiers⁵³, J Almond⁸², A Aloisio^{102a,102b}, R Alon¹⁷¹, A Alonso⁷⁹, M G Alviggi^{102a,102b}, K Amako⁶⁶, P Amaral²⁹, C Amelung²², V V Ammosov¹²⁸, A Amorim^{124a,179}, G Amorós¹⁶⁷, N Amram¹⁵³, C Anastopoulos¹³⁹, T Andeen³⁴, C F Anders²⁰, K J Anderson³⁰, A Andreazza^{89a,89b}, V Andrei^{58a}, M-L Andrieux⁵⁵, X S Anduaga⁷⁰, A Angerami³⁴, F Anghinolfi²⁹, N Anjos^{124a}, A Annovi⁴⁷, A Antonaki⁸, M Antonelli⁴⁷, S Antonelli^{19a,19b}, A Antonov⁹⁶, J Antos^{144b}, F Anulli^{132a}, S Aoun⁸³, L Aperiò Bella⁴, R Apolle¹¹⁸, G Arabidze⁸⁸, I Aracena¹⁴³, Y Arai⁶⁶, A T H Arce⁴⁴, J P Archambault²⁸, S Arfaoui^{29,180}, J-F Arguin¹⁴, E Arik^{18a,206}, M Arik^{18a}, A J Armbruster⁸⁷, O Arnaez⁸¹, C Arnault¹¹⁵, A Artamonov⁹⁵, G Artoni^{132a,132b}, D Arutinov²⁰, S Asai¹⁵⁵, R Asfandiyarov¹⁷², S Ask²⁷, B Åsman^{146a,146b}, L Asquith⁵, K Assamagan²⁴, A Astbury¹⁶⁹, A Astvatsatourov⁵², G Atoian¹⁷⁵, B Aubert⁴, B Auerbach¹⁷⁵, E Auge¹¹⁵, K Augsten¹²⁷, M Aourousseau^{145a}, N Austin⁷³, R Avramidou⁹, D Axen¹⁶⁸, C Ay⁵⁴, G Azuelos^{93,181}, Y Azuma¹⁵⁵, M A Baak²⁹, G Baccaglioni^{89a}, C Bacci^{134a,134b}, A M Bach¹⁴, H Bachacou¹³⁶, K Bachas²⁹, G Bachy²⁹, M Backes⁴⁹, M Backhaus²⁰, E Badescu^{25a}, P Bagnaia^{132a,132b}, S Bahinipati², Y Bai^{32a}, D C Bailey¹⁵⁸, T Bain¹⁵⁸, J T Baines¹²⁹, O K Baker¹⁷⁵, M D Baker²⁴, S Baker⁷⁷, F Baltasar Dos Santos Pedrosa²⁹, E Banas³⁸, P Banerjee⁹³, Sw Banerjee¹⁶⁹, D Banfi²⁹, A Bangert¹³⁷, V Bansal¹⁶⁹, H S Bansil¹⁷, L Barak¹⁷¹, S P Baranov⁹⁴, A Barashkou⁶⁵, A Barbaro Galtieri¹⁴, T Barber²⁷, E L Barberio⁸⁶, D Barberis^{50a,50b}, M Barbero²⁰, D Y Bardin⁶⁵, T Barillari⁹⁹, M Barisonzi¹⁷⁴, T Barklow¹⁴³, N Barlow²⁷, B M Barnett¹²⁹, R M Barnett¹⁴, A Baroncelli^{134a}, A J Barr¹¹⁸, F Barreiro⁸⁰, J Barreiro Guimarães da Costa⁵⁷, P Barrillon¹¹⁵, R Bartoldus¹⁴³, A E Barton⁷¹, D Bartsch²⁰, V Bartsch¹⁴⁹, R L Bates⁵³, L Batkova^{144a}, J R Batley²⁷, A Battaglia¹⁶, M Battistin²⁹, G Battistoni^{89a}, F Bauer¹³⁶, H S Bawa^{143,182}, B Beare¹⁵⁸, T Beau⁷⁸, P H Beauchemin¹¹⁸, R Beccherle^{50a}, P Bechtel⁴¹, H P Beck¹⁶, M Beckingham⁴⁸, K H Becks¹⁷⁴, A J Beddall^{18c}, A Beddall^{18c}, S Bedikian¹⁷⁵, V A Bednyakov⁶⁵, C P Bee⁸³, M Begel²⁴, S Behar Harpaz¹⁵², P K Behera⁶³, M Beimforde⁹⁹, C Belanger-Champagne¹⁶⁶, P J Bell⁴⁹, W H Bell⁴⁹, G Bella¹⁵³, L Bellagamba^{19a}, F Bellina²⁹, G Bellomo^{89a,89b}, M Bellomo^{119a}, A Belloni⁵⁷, O Beloborodova¹⁰⁷, K Belotskiy⁹⁶, O Beltramello²⁹, S Ben Ami¹⁵², O Benary¹⁵³, D Bencheekroun^{135a}, C Benchouk⁸³, M Bendel⁸¹, B H Benedict¹⁶³, N Benekos¹⁶⁵,

Y Benhammou¹⁵³, D P Benjamin⁴⁴, M Benoit¹¹⁵, J R Bensinger²², K Benslama¹³⁰, S Bentvelsen¹⁰⁵, D Berge²⁹, E Bergeaas Kuutmann⁴¹, N Berger⁴, F Berghaus¹⁶⁹, E Berglund⁴⁹, J Beringer¹⁴, K Bernardet⁸³, P Bernat⁷⁷, R Bernhard⁴⁸, C Bernius²⁴, T Berry⁷⁶, A Bertin^{19a,19b}, F Bertinelli²⁹, F Bertolucci^{122a,122b}, M I Besana^{89a,89b}, N Besson¹³⁶, S Bethke⁹⁹, W Bhimji⁴⁵, R M Bianchi²⁹, M Bianco^{72a,72b}, O Biebel⁹⁸, S P Bieniek⁷⁷, J Biesiada¹⁴, M Biglietti^{134a,134b}, H Bilokon⁴⁷, M Bindi^{19a,19b}, S Binet¹¹⁵, A Bingul^{18c}, C Bini^{132a,132b}, C Biscarat¹⁷⁷, U Bitenc⁴⁸, K M Black²¹, R E Blair⁵, J-B Blanchard¹¹⁵, G Blanchot²⁹, C Blocker²², J Blocki³⁸, A Blondel⁴⁹, W Blum⁸¹, U Blumenschein⁵⁴, G J Bobbink¹⁰⁵, V B Bobrovnikov¹⁰⁷, A Bocci⁴⁴, C R Boddy¹¹⁸, M Boehler⁴¹, J Boek¹⁷⁴, N Boelaert³⁵, S Böser⁷⁷, J A Bogaerts²⁹, A Bogdanchikov¹⁰⁷, A Bogouch^{90,206}, C Bohm^{146a}, V Boisvert⁷⁶, T Bold^{163,183}, V Boldea^{25a}, M Bona⁷⁵, V G Bondarenko⁹⁶, M Boonekamp¹³⁶, G Boorman⁷⁶, C N Booth¹³⁹, P Booth¹³⁹, S Bordoni⁷⁸, C Borer¹⁶, A Borisov¹²⁸, G Borissov⁷¹, I Borjanovic^{12a}, S Borroni^{132a,132b}, K Bos¹⁰⁵, D Boscherini^{19a}, M Bosman¹¹, H Boterenbrood¹⁰⁵, D Botterill¹²⁹, J Bouchami⁹³, J Boudreau¹²³, E V Bouhova-Thacker⁷¹, C Boulahouache¹²³, C Bourdarios¹¹⁵, N Bousson⁸³, A Boveia³⁰, J Boyd²⁹, I R Boyko⁶⁵, N I Bozhko¹²⁸, I Bozovic-Jelisavcic^{12b}, J Bracinik¹⁷, A Braem²⁹, E Brambilla^{72a,72b}, P Branchini^{134a}, G W Brandenburg⁵⁷, A Brandt⁷, G Brandt¹⁵, O Brandt⁵⁴, U Bratzler¹⁵⁶, B Brau⁸⁴, J E Brau¹¹⁴, H M Braun¹⁷⁴, B Brelrier¹⁵⁸, J Bremer²⁹, R Brenner¹⁶⁶, S Bressler¹⁵², D Breton¹¹⁵, N D Brett¹¹⁸, P G Bright-Thomas¹⁷, D Britton⁵³, F M Brochu²⁷, I Brock²⁰, R Brock⁸⁸, T J Brodbeck⁷¹, E Brodet¹⁵³, F Broggi^{89a}, C Bromberg⁸⁸, G Brooijmans³⁴, W K Brooks^{31b}, G Brown⁸², E Brubaker³⁰, P A Bruckman de Renstrom³⁸, D Bruncko^{144b}, R Bruneliere⁴⁸, S Brunet⁶¹, A Bruni^{19a}, G Bruni^{19a}, M Bruschi^{19a}, T Buanes¹³, F Bucci⁴⁹, J Buchanan¹¹⁸, N J Buchanan², P Buchholz¹⁴¹, R M Buckingham¹¹⁸, A G Buckley⁴⁵, S I Buda^{25a}, I A Budagov⁶⁵, B Budick¹⁰⁸, V Büscher⁸¹, L Bugge¹¹⁷, D Buirar-Clark¹¹⁸, E J Buis¹⁰⁵, O Bulekov⁹⁶, M Bunse⁴², T Buran¹¹⁷, H Burckhart²⁹, S Burdin⁷³, T Burgess¹³, S Burke¹²⁹, E Busato³³, P Bussey⁵³, C P Buszello¹⁶⁶, F Butin²⁹, B Butler¹⁴³, J M Butler²¹, C M Buttar⁵³, J M Butterworth⁷⁷, W Buttinger²⁷, T Byatt⁷⁷, S Cabrera Urbán¹⁶⁷, M Caccia^{89a,89b}, D Caforio^{19a,19b}, O Cakir^{3a}, P Calafiura¹⁴, G Calderini⁷⁸, P Calfayan⁹⁸, R Calkins¹⁰⁶, L P Caloba^{23a}, R Caloi^{132a,132b}, D Calvet³³, S Calvet³³, R Camacho Toro³³, A Camard⁷⁸, P Camarri^{133a,133b}, M Cambiaghi^{119a,119b}, D Cameron¹¹⁷, J Cammin²⁰, S Campana²⁹, M Campanelli⁷⁷, V Canale^{102a,102b}, F Canelli³⁰, A Canepa^{159a}, J Cantero⁸⁰, L Capasso^{102a,102b}, M D M Capeans Garrido²⁹, I Caprini^{25a}, M Caprini^{25a}, D Capriotti⁹⁹, M Capua^{36a,36b}, R Caputo¹⁴⁸, C Caramarcu^{25a}, R Cardarelli^{133a}, T Carli²⁹, G Carlino^{102a}, L Carminati^{89a,89b}, B Caron^{159a}, S Caron⁴⁸, C Carpentieri⁴⁸, G D Carrillo Montoya¹⁷², A A Carter⁷⁵, J R Carter²⁷, J Carvalho^{124a,184}, D Casadei¹⁰⁸, M P Casado¹¹, M Cascella^{122a,122b}, C Caso^{50a,50b,206}, A M Castaneda Hernandez¹⁷², E Castaneda-Miranda¹⁷², V Castillo Gimenez¹⁶⁷, N F Castro^{124a}, G Cataldi^{72a}, F Cataneo²⁹, A Catinaccio²⁹, J R Catmore⁷¹, A Cattai²⁹, G Cattani^{133a,133b}, S Caughron⁸⁸, D Cauz^{164a,164c}, A Cavallari^{132a,132b}, P Cavalleri⁷⁸, D Cavalli^{89a}, M Cavalli-Sforza¹¹, V Cavasinni^{122a,122b}, A Cazzato^{72a,72b}, F Ceradini^{134a,134b}, A S Cerqueira^{23a}, A Cerri²⁹, L Cerrito⁷⁵, F Cerutti⁴⁷, S A Cetin^{18b}, F Cevenini^{102a,102b}, A Chafaq^{135a}, D Chakraborty¹⁰⁶, K Chan², B Chapleau⁸⁵, J D Chapman²⁷, J W Chapman⁸⁷, E Chareyre⁷⁸, D G Charlton¹⁷, V Chavda⁸², S Cheatham⁷¹, S Chekanov⁵, S V Chekulaev^{159a}, G A Chelkov⁶⁵, M A Chelstowska¹⁰⁴, C Chen⁶⁴, H Chen²⁴, L Chen², S Chen^{32c}, T Chen^{32c}, X Chen¹⁷², S Cheng^{32a}, A Cheplakov⁶⁵, V F Chepurinov⁶⁵, R Cherkaoui El Moursli^{135e}, V Chernyatin²⁴, E Cheu⁶, S L Cheung¹⁵⁸, L Chevalier¹³⁶, F Chevallier¹³⁶, G Chiefari^{102a,102b}, L Chikovani⁵¹, J T Childers^{58a}, A Chilingarov⁷¹, G Chiodini^{72a}, M V Chizhov⁶⁵, G Choudalakis³⁰, S Chouridou¹³⁷, I A Christidi⁷⁷, A Christov⁴⁸, D Chromek-Burckhart²⁹, M L Chu¹⁵¹, J Chudoba¹²⁵, G Ciapetti^{132a,132b},

K Ciba³⁷, A K Ciftci^{3a}, R Ciftci^{3a}, D Cinca³³, V Cindro⁷⁴, M D Ciobotaru¹⁶³, C Ciocca^{19a,19b}, A Ciocio¹⁴, M Cirilli⁸⁷, M Ciubancan^{25a}, A Clark⁴⁹, P J Clark⁴⁵, W Cleland¹²³, J C Clemens⁸³, B Clement⁵⁵, C Clement^{146a,146b}, R W Clift¹²⁹, Y Coadou⁸³, M Cobal^{164a,164c}, A Coccaro^{50a,50b}, J Cochran⁶⁴, P Coe¹¹⁸, J G Cogan¹⁴³, J Coggeshall¹⁶⁵, E Cogneras¹⁷⁷, C D Cojocar²⁸, J Colas⁴, A P Colijn¹⁰⁵, C Collard¹¹⁵, N J Collins¹⁷, C Collins-Tooth⁵³, J Collot⁵⁵, G Colon⁸⁴, R Coluccia^{72a,72b}, G Comune⁸⁸, P Conde Muiño^{124a}, E Coniavitis¹¹⁸, M C Conidi¹¹, M Consonni¹⁰⁴, S Constantinescu^{25a}, C Conta^{119a,119b}, F Conventi^{102a,185}, J Cook²⁹, M Cooke¹⁴, B D Cooper⁷⁷, A M Cooper-Sarkar¹¹⁸, N J Cooper-Smith⁷⁶, K Copic³⁴, T Cornelissen^{50a,50b}, M Corradi^{19a}, F Corriveau^{85,186}, A Cortes-Gonzalez¹⁶⁵, G Cortiana⁹⁹, G Costa^{89a}, M J Costa¹⁶⁷, D Costanzo¹³⁹, T Costin³⁰, D Côte²⁹, R Coura Torres^{23a}, L Courneyea¹⁶⁹, G Cowan⁷⁶, C Cowden²⁷, B E Cox⁸², K Cranmer¹⁰⁸, F Crescioli^{122a,122b}, M Cristinziani²⁰, G Crosetti^{36a,36b}, R Crupi^{72a,72b}, S Crépe-Renaudin⁵⁵, C Cuenca Almenar¹⁷⁵, T Cuhadar Donszelmann¹³⁹, S Cuneo^{50a,50b}, M Curatolo⁴⁷, C J Curtis¹⁷, P Cwetanski⁶¹, H Czirr¹⁴¹, Z Czyczula¹¹⁷, S D'Auria⁵³, M D'Onofrio⁷³, A D'Orazio^{132a,132b}, A Da Rocha Gesualdi Mello^{23a}, P V M Da Silva^{23a}, C Da Via⁸², W Dabrowski³⁷, A Dahloff⁴⁸, T Dai⁸⁷, C Dallapiccola⁸⁴, S J Dallison^{129,206}, M Dam³⁵, M Dameri^{50a,50b}, D S Damiani¹³⁷, H O Danielsson²⁹, R Dankers¹⁰⁵, D Dannheim⁹⁹, V Dao⁴⁹, G Darbo^{50a}, G L Darlea^{25b}, C Daum¹⁰⁵, J P Dauvergne²⁹, W Davey⁸⁶, T Davidek¹²⁶, N Davidson⁸⁶, R Davidson⁷¹, M Davies⁹³, A R Davison⁷⁷, E Dawe¹⁴², I Dawson¹³⁹, J W Dawson^{5,206}, R K Daya³⁹, K De⁷, R de Asmundis^{102a}, S De Castro^{19a,19b}, P E De Castro Faria Salgado²⁴, S De Cecco⁷⁸, J de Graat⁹⁸, N De Groot¹⁰⁴, P de Jong¹⁰⁵, C De La Taille¹¹⁵, H De la Torre⁸⁰, B De Lotto^{164a,164c}, L De Mora⁷¹, L De Nooij¹⁰⁵, M De Oliveira Branco²⁹, D De Pedis^{132a}, P de Saintignon⁵⁵, A De Salvo^{132a}, U De Sanctis^{164a,164c}, A De Santo¹⁴⁹, J B De Vivie De Regie¹¹⁵, S Dean⁷⁷, D V Dedovich⁶⁵, J Degenhardt¹²⁰, M Dehchar¹¹⁸, M Deile⁹⁸, C Del Papa^{164a,164c}, J Del Peso⁸⁰, T Del Prete^{122a,122b}, A Dell'Acqua²⁹, L Dell'Asta^{89a,89b}, M Della Pietra^{102a,185}, D della Volpe^{102a,102b}, M Delmastro²⁹, P Delpierre⁸³, N Delruelle²⁹, P A Delsart⁵⁵, C Deluca¹⁴⁸, S Demers¹⁷⁵, M Demichev⁶⁵, B Demirkoz¹¹, J Deng¹⁶³, S P Denisov¹²⁸, D Derendarz³⁸, J E Derkaoui^{135d}, F Derue⁷⁸, P Dervan⁷³, K Desch²⁰, E Devetak¹⁴⁸, P O Deviveiros¹⁵⁸, A Dewhurst¹²⁹, B DeWilde¹⁴⁸, S Dhaliwal¹⁵⁸, R Dhullipudi^{24,187}, A Di Ciaccio^{133a,133b}, L Di Ciaccio⁴, A Di Girolamo²⁹, B Di Girolamo²⁹, S Di Luise^{134a,134b}, A Di Mattia⁸⁸, B Di Micco²⁹, R Di Nardo^{133a,133b}, A Di Simone^{133a,133b}, R Di Sipio^{19a,19b}, M A Diaz^{31a}, F Diblen^{18c}, E B Diehl⁸⁷, H Dietl⁹⁹, J Dietrich⁴⁸, T A Dietzsch^{58a}, S Diglio¹¹⁵, K Dindar Yagci³⁹, J Dingfelder²⁰, C Dionisi^{132a,132b}, P Dita^{25a}, S Dita^{25a}, F Dittus²⁹, F Djama⁸³, R Djilkibaev¹⁰⁸, T Djobava⁵¹, M A B do Vale^{23a}, A Do Valle Wemans^{124a}, T K O Doan⁴, M Dobbs⁸⁵, R Dobinson^{29,206}, D Dobos⁴², E Dobson²⁹, M Dobson¹⁶³, J Dodd³⁴, O B Dogan^{18a,206}, C Doglioni¹¹⁸, T Doherty⁵³, Y Doi^{66,206}, J Dolejsi¹²⁶, I Dolenc⁷⁴, Z Dolezal¹²⁶, B A Dolgoshein^{96,206}, T Dohmae¹⁵⁵, M Donadelli^{23b}, M Donega¹²⁰, J Donini⁵⁵, J Dopke²⁹, A Doria^{102a}, A Dos Anjos¹⁷², M Dosil¹¹, A Dotti^{122a,122b}, M T Dova⁷⁰, J D Dowell¹⁷, A D Doxiadis¹⁰⁵, A T Doyle⁵³, Z Drasal¹²⁶, J Drees¹⁷⁴, N Dressnandt¹²⁰, H Drevermann²⁹, C Driouichi³⁵, M Dris⁹, J G Drohan⁷⁷, J Dubbert⁹⁹, T Dubbs¹³⁷, S Dube¹⁴, E Duchovni¹⁷¹, G Duckeck⁹⁸, A Dudarev²⁹, F Dudziak⁶⁴, M Dührssen²⁹, I P Duerdoth⁸², L Duflot¹¹⁵, M-A Dufour⁸⁵, M Dunford²⁹, H Duran Yildiz^{3b}, R Duxfield¹³⁹, M Dwuznik³⁷, F Dydak²⁹, D Dzahini⁵⁵, M Düren⁵², W L Ebenstein⁴⁴, J Ebke⁹⁸, S Eckert⁴⁸, S Eckweiler⁸¹, K Edmonds⁸¹, C A Edwards⁷⁶, I Efthymiopoulos⁴⁹, W Ehrenfeld⁴¹, T Ehrich⁹⁹, T Eifert²⁹, G Eigen¹³, K Einsweiler¹⁴, E Eisenhandler⁷⁵, T Ekelof¹⁶⁶, M El Kacimi⁴, M Ellert¹⁶⁶, S Elles⁴, F Ellinghaus⁸¹, K Ellis⁷⁵, N Ellis²⁹, J Elmsheuser⁹⁸, M Elsing²⁹, R Ely¹⁴, D Emelianov¹²⁹, R Engelmann¹⁴⁸, A Engl⁹⁸, B Epp⁶², A Eppig⁸⁷, J Erdmann⁵⁴, A Ereditato¹⁶, D Eriksson^{146a}, J Ernst¹, M Ernst²⁴, J Ernwein¹³⁶, D Errede¹⁶⁵, S Errede¹⁶⁵, E Ertel⁸¹, M Escalier¹¹⁵, C Escobar¹⁶⁷,

X Espinal Curull¹¹, B Esposito⁴⁷, F Etienne⁸³, A I Etievre¹³⁶, E Etzion¹⁵³, D Evangelakou⁵⁴, H Evans⁶¹, L Fabbri^{19a,19b}, C Fabre²⁹, K Facius³⁵, R M Fakhrutdinov¹²⁸, S Falciano^{132a}, A C Falou¹¹⁵, Y Fang¹⁷², M Fanti^{89a,89b}, A Farbin⁷, A Farilla^{134a}, J Farley¹⁴⁸, T Farooque¹⁵⁸, S M Farrington¹¹⁸, P Farthouat²⁹, D Fasching¹⁷², P Fassnacht²⁹, D Fassouliotis⁸, B Fatholahzadeh¹⁵⁸, A Favareto^{89a,89b}, L Fayard¹¹⁵, S Fazio^{36a,36b}, R Febbraro³³, P Federic^{144a}, O L Fedin¹²¹, I Fedorko²⁹, W Fedorko⁸⁸, M Fehling-Kaschek⁴⁸, L Feligioni⁸³, D Fellmann⁵, C U Felzmann⁸⁶, C Feng^{32d}, E J Feng³⁰, A B Fenyuk¹²⁸, J Ferencei^{144b}, J Ferland⁹³, B Fernandes^{124a,179}, W Fernando¹⁰⁹, S Ferrag⁵³, J Ferrando¹¹⁸, V Ferrara⁴¹, A Ferrari¹⁶⁶, P Ferrari¹⁰⁵, R Ferrari^{119a}, A Ferrer¹⁶⁷, M L Ferrer⁴⁷, D Ferrere⁴⁹, C Ferretti⁸⁷, A Ferretto Parodi^{50a,50b}, M Fiascaris³⁰, F Fiedler⁸¹, A Filipčić⁷⁴, A Filippas⁹, F Filthaut¹⁰⁴, M Fincke-Keeler¹⁶⁹, M C N Fiolhais^{124a,184}, L Fiorini¹¹, A Firan³⁹, G Fischer⁴¹, P Fischer²⁰, M J Fisher¹⁰⁹, S M Fisher¹²⁹, J Flammer²⁹, M Flechl⁴⁸, I Fleck¹⁴¹, J Fleckner⁸¹, P Fleischmann¹⁷³, S Fleischmann¹⁷⁴, T Flick¹⁷⁴, L R Flores Castillo¹⁷², M J Flowerdew⁹⁹, F Föhlich^{58a}, M Fokitis⁹, T Fonseca Martin¹⁶, D A Forbush¹³⁸, A Formica¹³⁶, A Forti⁸², D Fortin^{159a}, J M Foster⁸², D Fournier¹¹⁵, A Foussat²⁹, A J Fowler⁴⁴, K Fowler¹³⁷, H Fox⁷¹, P Francavilla^{122a,122b}, S Franchino^{119a,119b}, D Francis²⁹, T Frank¹⁷¹, M Franklin⁵⁷, S Franz²⁹, M Fraternali^{119a,119b}, S Fratina¹²⁰, S T French²⁷, R Froeschl²⁹, D Froidevaux²⁹, J A Frost²⁷, C Fukunaga¹⁵⁶, E Fullana Torregrosa²⁹, J Fuster¹⁶⁷, C Gabaldon²⁹, O Gabizon¹⁷¹, T Gadfort²⁴, S Gadowski⁴⁹, G Gagliardi^{50a,50b}, P Gagnon⁶¹, C Galea⁹⁸, E J Gallas¹¹⁸, M V Gallas²⁹, V Gallo¹⁶, B J Gallop¹²⁹, P Gallus¹²⁵, E Galyaev⁴⁰, K K Gan¹⁰⁹, Y S Gao^{143,182}, V A Gapienko¹²⁸, A Gaponenko¹⁴, F Garberson¹⁷⁵, M Garcia-Sciveres¹⁴, C García¹⁶⁷, J E García Navarro⁴⁹, R W Gardner³⁰, N Garelli²⁹, H Garitaonandia¹⁰⁵, V Garonne²⁹, J Garvey¹⁷, C Gatti⁴⁷, G Gaudio^{119a}, O Gaumer⁴⁹, B Gaur¹⁴¹, L Gauthier¹³⁶, I L Gavrilenko⁹⁴, C Gay¹⁶⁸, G Gaycken²⁰, J-C Gayde²⁹, E N Gazis⁹, P Ge^{32d}, C N P Gee¹²⁹, D A A Geerts¹⁰⁵, Ch Geich-Gimbel²⁰, K Gellerstedt^{146a,146b}, C Gemme^{50a}, A Gemmell⁵³, M H Genest⁹⁸, S Gentile^{132a,132b}, M George⁵⁴, S George⁷⁶, P Gerlach¹⁷⁴, A Gershon¹⁵³, C Geweniger^{58a}, H Ghazlane^{135b}, P Ghez⁴, N Ghodbane³³, B Giacobbe^{19a}, S Giagu^{132a,132b}, V Giakoumopoulou⁸, V Giangiobbe^{122a,122b}, F Gianotti²⁹, B Gibbard²⁴, A Gibson¹⁵⁸, S M Gibson²⁹, G F Gieraltowski⁵, L M Gilbert¹¹⁸, M Gilchriese¹⁴, V Gilewsky⁹¹, D Gillberg²⁸, A R Gillman¹²⁹, D M Gingrich^{2,181}, J Ginzburg¹⁵³, N Giokaris⁸, R Giordano^{102a,102b}, F M Giorgi¹⁵, P Giovannini⁹⁹, P F Giraud¹³⁶, D Giugni^{89a}, P Giusti^{19a}, B K Gjelsten¹¹⁷, L K Gladilin⁹⁷, C Glasman⁸⁰, J Glatzer⁴⁸, A Glazov⁴¹, K W Glitza¹⁷⁴, G L Glonti⁶⁵, J Godfrey¹⁴², J Godlewski²⁹, M Goebel⁴¹, T Göpfert⁴³, C Goeringer⁸¹, C Gössling⁴², T Göttert⁹⁹, S Goldfarb⁸⁷, D Goldin³⁹, T Golling¹⁷⁵, S N Golovnia¹²⁸, A Gomes^{124a,179}, L S Gomez Fajardo⁴¹, R Gonçalo⁷⁶, J Goncalves Pinto Firmino Da Costa⁴¹, L Gonella²⁰, A Gonidec²⁹, S Gonzalez¹⁷², S González de la Hoz¹⁶⁷, M L Gonzalez Silva²⁶, S Gonzalez-Sevilla⁴⁹, J J Goodson¹⁴⁸, L Goossens²⁹, P A Gorbounov⁹⁵, H A Gordon²⁴, I Gorelov¹⁰³, G Gorfine¹⁷⁴, B Gorini²⁹, E Gorini^{72a,72b}, A Gorišek⁷⁴, E Gornicki³⁸, S A Gorokhov¹²⁸, V N Goryachev¹²⁸, B Gosdzik⁴¹, M Gosselink¹⁰⁵, M I Gostkin⁶⁵, M Gouanère⁴, I Gough Eschrich¹⁶³, M Gouighri^{135a}, D Goujdami^{135a}, M P Goulette⁴⁹, A G Goussiou¹³⁸, C Goy⁴, I Grabowska-Bold^{163,183}, V Grabski¹⁷⁶, P Grafström²⁹, C Grah¹⁷⁴, K-J Grahn¹⁴⁷, F Grancagnolo^{72a}, S Grancagnolo¹⁵, V Grassi¹⁴⁸, V Gratchev¹²¹, N Grau³⁴, H M Gray²⁹, J A Gray¹⁴⁸, E Graziani^{134a}, O G Grebenyuk¹²¹, D Greenfield¹²⁹, T Greenshaw⁷³, Z D Greenwood^{24,187}, I M Gregor⁴¹, P Grenier¹⁴³, E Griesmayer⁴⁶, J Griffiths¹³⁸, N Grigalashvili⁶⁵, A A Grillo¹³⁷, S Grinstein¹¹, P L Y Gris³³, Y V Grishkevich⁹⁷, J-F Grivaz¹¹⁵, J Grognuz²⁹, M Groh⁹⁹, E Gross¹⁷¹, J Grosse-Knetter⁵⁴, J Groth-Jensen⁷⁹, M Gruwe²⁹, K Grybel¹⁴¹, V J Guarino⁵, D Guest¹⁷⁵, C Guicheney³³, A Guida^{72a,72b}, T Guillemin⁴, S Guindon⁵⁴, H Guler^{85,188}, J Gunther¹²⁵, B Guo¹⁵⁸, J Guo³⁴, A Gupta³⁰, Y Gusakov⁶⁵, V N Gushchin¹²⁸, A Gutierrez⁹³,

P Gutierrez¹¹¹, N Guttman¹⁵³, O Gutzwiller¹⁷², C Guyot¹³⁶, C Gwenlan¹¹⁸, C B Gwilliam⁷³, A Haas¹⁴³, S Haas²⁹, C Haber¹⁴, R Hackenburg²⁴, H K Hadavand³⁹, D R Hadley¹⁷, P Haefner⁹⁹, F Hahn²⁹, S Haider²⁹, Z Hajduk³⁸, H Hakobyan¹⁷⁶, J Haller⁵⁴, K Hamacher¹⁷⁴, P Hamal¹¹³, A Hamilton⁴⁹, S Hamilton¹⁶¹, H Han^{32a}, L Han^{32b}, K Hanagaki¹¹⁶, M Hance¹²⁰, C Handel⁸¹, P Hanke^{58a}, C J Hansen¹⁶⁶, J R Hansen³⁵, J B Hansen³⁵, J D Hansen³⁵, P H Hansen³⁵, P Hansson¹⁴³, K Hara¹⁶⁰, G A Hare¹³⁷, T Harenberg¹⁷⁴, D Harper⁸⁷, R D Harrington²¹, O M Harris¹³⁸, K Harrison¹⁷, J Hartert⁴⁸, F Hartjes¹⁰⁵, T Haruyama⁶⁶, A Harvey⁵⁶, S Hasegawa¹⁰¹, Y Hasegawa¹⁴⁰, S Hassani¹³⁶, M Hatch²⁹, D Hauff⁹⁹, S Haug¹⁶, M Hauschild²⁹, R Hauser⁸⁸, M Havranek²⁰, B M Hawes¹¹⁸, C M Hawkes¹⁷, R J Hawkings²⁹, D Hawkins¹⁶³, T Hayakawa⁶⁷, D Hayden⁷⁶, H S Hayward⁷³, S J Haywood¹²⁹, E Hazen²¹, M He^{32d}, S J Head¹⁷, V Hedberg⁷⁹, L Heelan⁷, S Heim⁸⁸, B Heinemann¹⁴, S Heisterkamp³⁵, L Helary⁴, M Heldmann⁴⁸, M Heller¹¹⁵, S Hellman^{146a,146b}, C Hensens¹¹, R C W Henderson⁷¹, M Henke^{58a}, A Henrichs⁵⁴, A M Henriques Correia²⁹, S Henrot-Versille¹¹⁵, F Henry-Couannier⁸³, C Hensel⁵⁴, T Henß¹⁷⁴, Y Hernández Jiménez¹⁶⁷, R Herrberg¹⁵, A D Hershenhorn¹⁵², G Herten⁴⁸, R Hertenberger⁹⁸, L Hervas²⁹, N P Hessey¹⁰⁵, A Hidvegi^{146a}, E Higón-Rodríguez¹⁶⁷, D Hill^{5,206}, J C Hill²⁷, N Hill⁵, K H Hiller⁴¹, S Hillert²⁰, S J Hillier¹⁷, I Hinchliffe¹⁴, E Hines¹²⁰, M Hirose¹¹⁶, F Hirsch⁴², D Hirschbuehl¹⁷⁴, J Hobbs¹⁴⁸, N Hod¹⁵³, M C Hodgkinson¹³⁹, P Hodgson¹³⁹, A Hoecker²⁹, M R Hoferkamp¹⁰³, J Hoffman³⁹, D Hoffmann⁸³, M Hohlfeld⁸¹, M Holder¹⁴¹, A Holmes¹¹⁸, S O Holmgren^{146a}, T Holy¹²⁷, J L Holzbauer⁸⁸, Y Homma⁶⁷, L Hooft van Huysduynen¹⁰⁸, T Horazdovsky¹²⁷, C Horn¹⁴³, S Horner⁴⁸, K Horton¹¹⁸, J-Y Hostachy⁵⁵, T Hott⁹⁹, S Hou¹⁵¹, M A Houlden⁷³, A Hoummada^{135a}, J Howarth⁸², D F Howell¹¹⁸, I Hristova⁴¹, J Hrivnac¹¹⁵, I Hruska¹²⁵, T Hryn'ova⁴, P J Hsu¹⁷⁵, S-C Hsu¹⁴, G S Huang¹¹¹, Z Hubacek¹²⁷, F Hubaut⁸³, F Huegging²⁰, T B Huffman¹¹⁸, E W Hughes³⁴, G Hughes⁷¹, R E Hughes-Jones⁸², M Huhtinen²⁹, P Hurst⁵⁷, M Hurwitz¹⁴, U Husemann⁴¹, N Huseynov^{65,189}, J Huston⁸⁸, J Huth⁵⁷, G Iacobucci^{102a}, G Iakovidis⁹, M Ibbotson⁸², I Ibragimov¹⁴¹, R Ichimiya⁶⁷, L Iconomidou-Fayard¹¹⁵, J Idarraga¹¹⁵, M Idzik³⁷, P Iengo⁴, O Igonkina¹⁰⁵, Y Ikegami⁶⁶, M Ikeno⁶⁶, Y Ilchenko³⁹, D Iliadis¹⁵⁴, D Imbault⁷⁸, M Imhaeuser¹⁷⁴, M Imori¹⁵⁵, T Ince²⁰, J Inigo-Golfin²⁹, P Ioannou⁸, M Iodice^{134a}, G Ionescu⁴, A Irls Quiles¹⁶⁷, K Ishii⁶⁶, A Ishikawa⁶⁷, M Ishino⁶⁶, R Ishmukhametov³⁹, C Issever¹¹⁸, S Istin^{18a}, Y Itoh¹⁰¹, A V Ivashin¹²⁸, W Iwanski³⁸, H Iwasaki⁶⁶, J M Izen⁴⁰, V Izzo^{102a}, B Jackson¹²⁰, J N Jackson⁷³, P Jackson¹⁴³, M R Jaekel²⁹, V Jain⁶¹, K Jakobs⁴⁸, S Jakobsen³⁵, J Jakubek¹²⁷, D K Jana¹¹¹, E Jankowski¹⁵⁸, E Jansen⁷⁷, A Jantsch⁹⁹, M Janus²⁰, G Jarlskog⁷⁹, L Jeanty⁵⁷, K Jelen³⁷, I Jen-La Plante³⁰, P Jenni²⁹, A Jeremie⁴, P Jež³⁵, S Jézéquel⁴, M K Jha^{19a}, H Ji¹⁷², W Ji⁸¹, J Jia¹⁴⁸, Y Jiang^{32b}, M Jimenez Belenguer⁴¹, G Jin^{32b}, S Jin^{32a}, O Jinnouchi¹⁵⁷, M D Joergensen³⁵, D Joffe³⁹, L G Johansen¹³, M Johansen^{146a,146b}, K E Johansson^{146a}, P Johansson¹³⁹, S Johnert⁴¹, K A Johns⁶, K Jon-And^{146a,146b}, G Jones⁸², R W L Jones⁷¹, T W Jones⁷⁷, T J Jones⁷³, O Jonsson²⁹, C Joram²⁹, P M Jorge^{124a,179}, J Joseph¹⁴, X Ju¹³⁰, V Juranek¹²⁵, P Jussel⁶², V V Kabachenko¹²⁸, S Kabana¹⁶, M Kaci¹⁶⁷, A Kaczmarska³⁸, P Kadlecik³⁵, M Kado¹¹⁵, H Kagan¹⁰⁹, M Kagan⁵⁷, S Kaiser⁹⁹, E Kajomovitz¹⁵², S Kalinin¹⁷⁴, L V Kalinovskaya⁶⁵, S Kama³⁹, N Kanaya¹⁵⁵, M Kaneda¹⁵⁵, T Kanno¹⁵⁷, V A Kantserov⁹⁶, J Kanzaki⁶⁶, B Kaplan¹⁷⁵, A Kapliy³⁰, J Kaplon²⁹, D Kar⁴³, M Karagoz¹¹⁸, M Karnevskiy⁴¹, K Kari⁵, V Kartvelishvili⁷¹, A N Karyukhin¹²⁸, L Kashif¹⁷², A Kasmi³⁹, R D Kass¹⁰⁹, A Kastanas¹³, M Kataoka⁴, Y Kataoka¹⁵⁵, E Katsoufis⁹, J Katzy⁴¹, V Kaushik⁶, K Kawagoe⁶⁷, T Kawamoto¹⁵⁵, G Kawamura⁸¹, M S Kayl¹⁰⁵, V A Kazanin¹⁰⁷, M Y Kazarinov⁶⁵, S I Kazi⁸⁶, J R Keates⁸², R Keeler¹⁶⁹, R Kehoe³⁹, M Keil⁵⁴, G D Kekelidze⁶⁵, M Kelly⁸², J Kennedy⁹⁸, C J Kenney¹⁴³, M Kenyon⁵³, O Kepka¹²⁵, N Kerschen²⁹, B P Kerševan⁷⁴, S Kersten¹⁷⁴, K Kessoku¹⁵⁵, C Ketterer⁴⁸, M Khakzad²⁸, F Khalilzada¹⁰, H Khandanyan¹⁶⁵, A Khanov¹¹², D Kharchenko⁶⁵, A Khodinov¹⁴⁸, A G Kholodenko¹²⁸,

A Khomich^{58a}, T J Khoo²⁷, G Khoriali²⁰, N Khovanskiy⁶⁵, V Khovanskiy⁹⁵, E Khramov⁶⁵, J Khubua⁵¹, G Kilvington⁷⁶, H Kim⁷, M S Kim², P C Kim¹⁴³, S H Kim¹⁶⁰, N Kimura¹⁷⁰, O Kind¹⁵, B T King⁷³, M King⁶⁷, R S B King¹¹⁸, J Kirk¹²⁹, G P Kirsch¹¹⁸, L E Kirsch²², A E Kiryunin⁹⁹, D Kisiielewska³⁷, T Kittelmann¹²³, A M Kiver¹²⁸, H Kiyamura⁶⁷, E Kladiva^{144b}, J Klaiber-Lodewigs⁴², M Klein⁷³, U Klein⁷³, K Kleinknecht⁸¹, M Klemetti⁸⁵, A Klier¹⁷¹, A Klimentov²⁴, R Klingenberg⁴², E B Klinkby³⁵, T Klioutchnikova²⁹, P F Klok¹⁰⁴, S Klous¹⁰⁵, E -E Kluge^{58a}, T Kluge⁷³, P Kluit¹⁰⁵, S Kluth⁹⁹, E Kneringer⁶², J Knobloch²⁹, E B F G Knoops⁸³, A Knue⁵⁴, B R Ko⁴⁴, T Kobayashi¹⁵⁵, M Kobel⁴³, B Koblitz²⁹, M Kocian¹⁴³, A Kocnar¹¹³, P Kodys¹²⁶, K Köneke²⁹, A C König¹⁰⁴, S Koenig⁸¹, S König⁴⁸, L Köpke⁸¹, F Koetsveld¹⁰⁴, P Koevesarki²⁰, T Koffas²⁹, E Koffeman¹⁰⁵, F Kohn⁵⁴, Z Kohout¹²⁷, T Kohriki⁶⁶, T Koi¹⁴³, T Kokott²⁰, G M Kolachev¹⁰⁷, H Kolanoski¹⁵, V Kolesnikov⁶⁵, I Koletsou^{89a}, J Koll⁸⁸, D Kollar²⁹, M Kollefrath⁴⁸, S D Kolya⁸², A A Komar⁹⁴, J R Komaragiri¹⁴², T Kondo⁶⁶, T Kono^{41,190}, A I Kononov⁴⁸, R Konoplich^{108,191}, N Konstantinidis⁷⁷, A Kootz¹⁷⁴, S Koperny³⁷, S V Kopikov¹²⁸, K Korcyl³⁸, K Kordas¹⁵⁴, V Koreshev¹²⁸, A Korn¹⁴, A Korol¹⁰⁷, I Korolkov¹¹, E V Korolkova¹³⁹, V A Korotkov¹²⁸, O Kortner⁹⁹, S Kortner⁹⁹, V V Kostyukhin²⁰, M J Kotamäki²⁹, S Kotov⁹⁹, V M Kotov⁶⁵, C Kourkoumelis⁸, V Kouskoura¹⁵⁴, A Koutsman¹⁰⁵, R Kowalewski¹⁶⁹, T Z Kowalski³⁷, W Kozanecki¹³⁶, A S Kozhin¹²⁸, V Kral¹²⁷, V A Kramarenko⁹⁷, G Kramberger⁷⁴, O Krasel⁴², M W Krasny⁷⁸, A Krasznahorkay¹⁰⁸, J Kraus⁸⁸, A Kreisel¹⁵³, F Krejci¹²⁷, J Kretzschmar⁷³, N Krieger⁵⁴, P Krieger¹⁵⁸, K Kroeninger⁵⁴, H Kroha⁹⁹, J Kroll¹²⁰, J Kroseberg²⁰, J Krstic^{12a}, U Kruchonak⁶⁵, H Krüger²⁰, Z V Krumshiteyn⁶⁵, A Kruth²⁰, T Kubota¹⁵⁵, S Kuehn⁴⁸, A Kugel^{58c}, T Kuhl¹⁷⁴, D Kuhn⁶², V Kukhtin⁶⁵, Y Kulchitsky⁹⁰, S Kuleshov^{31b}, C Kummer⁹⁸, M Kuna⁷⁸, N Kundu¹¹⁸, J Kunkle¹²⁰, A Kupco¹²⁵, H Kurashige⁶⁷, M Kurata¹⁶⁰, Y A Kurochkin⁹⁰, V Kus¹²⁵, W Kuykendall¹³⁸, M Kuze¹⁵⁷, P Kuzhir⁹¹, O Kvasnicka¹²⁵, J Kvita²⁹, R Kwee¹⁵, A La Rosa²⁹, L La Rotonda^{36a,36b}, L Labarga⁸⁰, J Labbe⁴, S Lablak^{135a}, C Lacasta¹⁶⁷, F Lacava^{132a,132b}, H Lacker¹⁵, D Lacour⁷⁸, V R Lacuesta¹⁶⁷, E Ladygin⁶⁵, R Lafaye⁴, B Laforge⁷⁸, T Lagouri⁸⁰, S Lai⁴⁸, E Laisne⁵⁵, M Lamanna²⁹, C L Lampen⁶, W Lamp⁶, E Lancon¹³⁶, U Landgraf⁴⁸, M P J Landon⁷⁵, H Landsman¹⁵², J L Lane⁸², C Lange⁴¹, A J Lankford¹⁶³, F Lanni²⁴, K Lantzsch²⁹, V V Lapin^{128,206}, S Laplace⁷⁸, C Lapoire²⁰, J F Laporte¹³⁶, T Lari^{89a}, A V Larionov¹²⁸, A Lerner¹¹⁸, C Lasseur²⁹, M Lassnig²⁹, W Lau¹¹⁸, P Laurelli⁴⁷, A Lavorato¹¹⁸, W Lavrijsen¹⁴, P Laycock⁷³, A B Lazarev⁶⁵, A Lazzaro^{89a,89b}, O Le Dortz⁷⁸, E Le Guirriec⁸³, C Le Maner¹⁵⁸, E Le Menedeu¹³⁶, M Leahu²⁹, A Lebedev⁶⁴, C Lebel⁹³, T LeCompte⁵, F Ledroit-Guillon⁵⁵, H Lee¹⁰⁵, J S H Lee¹⁵⁰, S C Lee¹⁵¹, L Lee¹⁷⁵, M Lefebvre¹⁶⁹, M Legendre¹³⁶, A Leger⁴⁹, B C LeGeyt¹²⁰, F Legger⁹⁸, C Leggett¹⁴, M Lehmacher²⁰, G Lehmann Miotto²⁹, X Lei⁶, M A L Leite^{23b}, R Leitner¹²⁶, D Lellouch¹⁷¹, J Lellouch⁷⁸, M Leltchouk³⁴, V Lendermann^{58a}, K J C Leney^{145b}, T Lenz¹⁷⁴, G Lenzen¹⁷⁴, B Lenzi¹³⁶, K Leonhardt⁴³, S Leontsinis⁹, C Leroy⁹³, J-R Lessard¹⁶⁹, J Lesser^{146a}, C G Lester²⁷, A Leung Fook Cheong¹⁷², J Levêque⁴, D Levin⁸⁷, L J Levinson¹⁷¹, M S Levitski¹²⁸, M Lewandowska²¹, G H Lewis¹⁰⁸, M Leyton¹⁵, B Li⁸³, H Li¹⁷², S Li^{32b}, X Li⁸⁷, Z Liang³⁹, Z Liang^{118,192}, B Liberti^{133a}, P Lichard²⁹, M Lichtnecker⁹⁸, K Lie¹⁶⁵, W Liebig¹³, R Lifshitz¹⁵², J N Lilley¹⁷, C Limbach²⁰, A Limosani⁸⁶, M Limper⁶³, S C Lin^{151,193}, F Linde¹⁰⁵, J T Linnemann⁸⁸, E Lipeles¹²⁰, L Lipinsky¹²⁵, A Lipniacka¹³, T M Liss¹⁶⁵, D Lissauer²⁴, A Lister⁴⁹, A M Litke¹³⁷, C Liu²⁸, D Liu^{151,194}, H Liu⁸⁷, J B Liu⁸⁷, M Liu^{32b}, S Liu², Y Liu^{32b}, M Livan^{119a,119b}, S S A Livermore¹¹⁸, A Lleres⁵⁵, S L Lloyd⁷⁵, E Lobodzinska⁴¹, P Loch⁶, W S Lockman¹³⁷, S Lockwitz¹⁷⁵, T Loddenkoetter²⁰, F K Loebinger⁸², A Loginov¹⁷⁵, C W Loh¹⁶⁸, T Lohse¹⁵, K Lohwasser⁴⁸, M Lokajicek¹²⁵, J Loken¹¹⁸, V P Lombardo^{89a}, R E Long⁷¹, L Lopes^{124a,179}, D Lopez Mateos^{34,195}, M Losada¹⁶², P Loscutoff¹⁴, F Lo Sterzo^{132a,132b}, M J Losty^{159a}, X Lou⁴⁰, A Lounis¹¹⁵, K F Loureiro¹⁶²,

J Love²¹, P A Love⁷¹, A J Lowe^{143,182}, F Lu^{32a}, J Lu², L Lu³⁹, H J Lubatti¹³⁸, C Luci^{132a,132b}, A Lucotte⁵⁵, A Ludwig⁴³, D Ludwig⁴¹, I Ludwig⁴⁸, J Ludwig⁴⁸, F Luehring⁶¹, G Luijckx¹⁰⁵, D Lumb⁴⁸, L Luminari^{132a}, E Lund¹¹⁷, B Lund-Jensen¹⁴⁷, B Lundberg⁷⁹, J Lundberg^{146a,146b}, J Lundquist³⁵, M Lungwitz⁸¹, A Lupi^{122a,122b}, G Lutz⁹⁹, D Lynn²⁴, J Lys¹⁴, E Lytken⁷⁹, H Ma²⁴, L L Ma¹⁷², J A Macana Goia⁹³, G Maccarrone⁴⁷, A Macchiolo⁹⁹, B Maček⁷⁴, J Machado Miguens^{124a}, D Macina⁴⁹, R Mackeprang³⁵, R J Madaras¹⁴, W F Mader⁴³, R Maenner^{58c}, T Maeno²⁴, P Mättig¹⁷⁴, S Mättig⁴¹, P J Magalhaes Martins^{124a,184}, L Magnoni²⁹, E Magradze⁵¹, C A Magrath¹⁰⁴, Y Mahalalel¹⁵³, K Mahboubi⁴⁸, G Mahout¹⁷, C Maiani^{132a,132b}, C Maidantchik^{23a}, A Maio^{124a,179}, S Majewski²⁴, Y Makida⁶⁶, N Makovec¹¹⁵, P Mal⁶, Pa Malecki³⁸, P Malecki³⁸, V P Maleev¹²¹, F Malek⁵⁵, U Mallik⁶³, D Malon⁵, S Maltezos⁹, V Malyshev¹⁰⁷, S Malyukov⁶⁵, R Mameghani⁹⁸, J Mamuzic^{12b}, A Manabe⁶⁶, L Mandelli^{89a}, I Mandić⁷⁴, R Mandrysch¹⁵, J Maneira^{124a}, P S Mangeard⁸⁸, I D Manjavidze⁶⁵, A Mann⁵⁴, P M Manning¹³⁷, A Manousakis-Katsikakis⁸, B Mansoulie¹³⁶, A Manz⁹⁹, A Mapelli²⁹, L Mapelli²⁹, L March⁸⁰, J F Marchand²⁹, F Marchese^{133a,133b}, M Marchesotti²⁹, G Marchiori⁷⁸, M Marcisovsky¹²⁵, A Marin^{21,206}, C P Marino⁶¹, F Marroquim^{23a}, R Marshall⁸², Z Marshall^{34,195}, F K Martens¹⁵⁸, S Marti-Garcia¹⁶⁷, A J Martin¹⁷⁵, B Martin²⁹, B Martin⁸⁸, F F Martin¹²⁰, J P Martin⁹³, Ph Martin⁵⁵, T A Martin¹⁷, B Martin dit Latour⁴⁹, M Martinez¹¹, V Martinez Outschoorn⁵⁷, A C Martyniuk⁸², M Marx⁸², F Marzano^{132a}, A Marzin¹¹¹, L Masetti⁸¹, T Mashimo¹⁵⁵, R Mashinistov⁹⁴, J Masik⁸², A L Maslennikov¹⁰⁷, M Maß⁴², I Massa^{19a,19b}, G Massaro¹⁰⁵, N Massol⁴, A Mastroberardino^{36a,36b}, T Masubuchi¹⁵⁵, M Mathes²⁰, P Matricon¹¹⁵, H Matsumoto¹⁵⁵, H Matsunaga¹⁵⁵, T Matsushita⁶⁷, C Matravers^{118,196}, J M Maugain²⁹, S J Maxfield⁷³, D A Maximov¹⁰⁷, E N May⁵, A Mayne¹³⁹, R Mazini¹⁵¹, M Mazur²⁰, M Mazzanti^{89a}, E Mazzoni^{122a,122b}, S P Mc Kee⁸⁷, A McCarn¹⁶⁵, R L McCarthy¹⁴⁸, T G McCarthy²⁸, N A McCubbin¹²⁹, K W McFarlane⁵⁶, J A Mcfayden¹³⁹, H McGlone⁵³, G Mchedlidze⁵¹, R A McLaren²⁹, T Mclaughlan¹⁷, S J McMahan¹²⁹, R A McPherson^{169,186}, A Meade⁸⁴, J Mechnich¹⁰⁵, M Mechtel¹⁷⁴, M Medinnis⁴¹, R Meera-Lebbai¹¹¹, T Meguro¹¹⁶, R Mehdiyev⁹³, S Mehlhase³⁵, A Mehta⁷³, K Meier^{58a}, J Meinhardt⁴⁸, B Meirose⁷⁹, C Melachrinou³⁰, B R Mellado Garcia¹⁷², L Mendoza Navas¹⁶², Z Meng^{151,194}, A Mengarelli^{19a,19b}, S Menke⁹⁹, C Menot²⁹, E Meoni¹¹, K M Mercurio⁵⁷, P Mermod¹¹⁸, L Merola^{102a,102b}, C Meroni^{89a}, F S Merritt³⁰, A Messina²⁹, J Metcalfe¹⁰³, A S Mete⁶⁴, S Meuser²⁰, C Meyer⁸¹, J-P Meyer¹³⁶, J Meyer¹⁷³, J Meyer⁵⁴, T C Meyer²⁹, W T Meyer⁶⁴, J Miao^{32d}, S Michal²⁹, L Micu^{25a}, R P Middleton¹²⁹, P Miele²⁹, S Migas⁷³, L Mijović⁴¹, G Mikenberg¹⁷¹, M Mikestikova¹²⁵, B Mikulec⁴⁹, M Mikuž⁷⁴, D W Miller¹⁴³, R J Miller⁸⁸, W J Mills¹⁶⁸, C Mills⁵⁷, A Milov¹⁷¹, D A Milstead^{146a,146b}, D Milstein¹⁷¹, A A Minaenko¹²⁸, M Miñano¹⁶⁷, I A Minashvili⁶⁵, A I Mincer¹⁰⁸, B Mindur³⁷, M Mineev⁶⁵, Y Ming¹³⁰, L M Mir¹¹, G Mirabelli^{132a}, L Miralles Verge¹¹, A Misiejuk⁷⁶, J Mitrevski¹³⁷, G Y Mitrofanov¹²⁸, V A Mitsou¹⁶⁷, S Mitsui⁶⁶, P S Miyagawa⁸², K Miyazaki⁶⁷, J U Mjörnmark⁷⁹, T Moa^{146a,146b}, P Mockett¹³⁸, S Moed⁵⁷, V Moeller²⁷, K Mönig⁴¹, N Möser²⁰, S Mohapatra¹⁴⁸, B Mohn¹³, W Mohr⁴⁸, S Mohr dieck-Möck⁹⁹, A M Moisseev^{128,206}, R Moles-Valls¹⁶⁷, J Molina-Perez²⁹, L Moneta⁴⁹, J Monk⁷⁷, E Monnier⁸³, S Montesano^{89a,89b}, F Monticelli⁷⁰, S Monzani^{19a,19b}, R W Moore², G F Moorhead⁸⁶, C Mora Herrera⁴⁹, A Moraes⁵³, A Morais^{124a,179}, N Morange¹³⁶, G Morello^{36a,36b}, D Moreno⁸¹, M Moreno Llácer¹⁶⁷, P Morettini^{50a}, M Morii⁵⁷, J Morin⁷⁵, Y Morita⁶⁶, A K Morley²⁹, G Mornacchi²⁹, M-C Morone⁴⁹, S V Morozov⁹⁶, J D Morris⁷⁵, H G Moser⁹⁹, M Mosidze⁵¹, J Moss¹⁰⁹, R Mount¹⁴³, E Mountricha⁹, S V Mouraviev⁹⁴, E J W Moyses⁸⁴, M Mudrinic^{12b}, F Mueller^{58a}, J Mueller¹²³, K Mueller²⁰, T A Müller⁹⁸, D Muenstermann²⁹, A Muijs¹⁰⁵, A Muir¹⁶⁸, Y Munwes¹⁵³, K Murakami⁶⁶, W J Murray¹²⁹, I Mussche¹⁰⁵, E Musto^{102a,102b}, A G Myagkov¹²⁸, M Myska¹²⁵, J Nadal¹¹, K Nagai¹⁶⁰, K Nagano⁶⁶, Y Nagasaka⁶⁰, A M Nairz²⁹,

Y Nakahama¹¹⁵, K Nakamura¹⁵⁵, I Nakano¹¹⁰, G Nanava²⁰, A Napier¹⁶¹, M Nash^{77,196}, N R Nation²¹, T Nattermann²⁰, T Naumann⁴¹, G Navarro¹⁶², H A Neal⁸⁷, E Nebot⁸⁰, P Yu Nechaeva⁹⁴, A Negri^{119a,119b}, G Negri²⁹, S Nektarijevic⁴⁹, A Nelson⁶⁴, S Nelson¹⁴³, T K Nelson¹⁴³, S Nemecek¹²⁵, P Nemethy¹⁰⁸, A A Nepomuceno^{23a}, M Nessi^{29,197}, S Y Nesterov¹²¹, M S Neubauer¹⁶⁵, A Neusiedl⁸¹, R M Neves¹⁰⁸, P Nevski²⁴, P R Newman¹⁷, R B Nickerson¹¹⁸, R Nicolaidou¹³⁶, L Nicolas¹³⁹, B Nicquevert²⁹, F Niedercorn¹¹⁵, J Nielsen¹³⁷, T Niinikoski²⁹, A Nikiforov¹⁵, V Nikolaenko¹²⁸, K Nikolaev⁶⁵, I Nikolic-Audit⁷⁸, K Nikolopoulos²⁴, H Nilsen⁴⁸, P Nilsson⁷, Y Ninomiya¹⁵⁵, A Nisati^{132a}, T Nishiyama⁶⁷, R Nisius⁹⁹, L Nodulman⁵, M Nomachi¹¹⁶, I Nomidis¹⁵⁴, H Nomoto¹⁵⁵, M Nordberg²⁹, B Nordkvist^{146a,146b}, P R Norton¹²⁹, J Novakova¹²⁶, M Nozaki⁶⁶, M Nožička⁴¹, L Nozka¹¹³, I M Nugent^{159a}, A-E Nuncio-Quiroz²⁰, G Nunes Hanninger²⁰, T Nunnemann⁹⁸, E Nurse⁷⁷, T Nyman²⁹, B J O'Brien⁴⁵, S W O'Neale^{17,206}, D C O'Neil¹⁴², V O'Shea⁵³, F G Oakham^{28,181}, H Oberlack⁹⁹, J Ocariz⁷⁸, A Ochi⁶⁷, S Oda¹⁵⁵, S Odaka⁶⁶, J Odier⁸³, H Ogren⁶¹, A Oh⁸², S H Oh⁴⁴, C C Ohm^{146a,146b}, T Ohshima¹⁰¹, H Ohshita¹⁴⁰, T K Ohska⁶⁶, T Ohsugi⁵⁹, S Okada⁶⁷, H Okawa¹⁶³, Y Okumura¹⁰¹, T Okuyama¹⁵⁵, M Olcese^{50a}, A G Olchevski⁶⁵, M Oliveira^{124a,184}, D Oliveira Damazio²⁴, E Oliver Garcia¹⁶⁷, D Olivito¹²⁰, A Olszewski³⁸, J Olszowska³⁸, C Omachi⁶⁷, A Onofre^{124a,198}, P U E Onyisi³⁰, C J Oram^{159a}, G Ordonez¹⁰⁴, M J Oreglia³⁰, F Orellana⁴⁹, Y Oren¹⁵³, D Orestano^{134a,134b}, I Orlov¹⁰⁷, C Oropeza Barrera⁵³, R S Orr¹⁵⁸, E O Ortega¹³⁰, B Osculati^{50a,50b}, R Ospanov¹²⁰, C Osuna¹¹, G Otero y Garzon²⁶, J P Ottersbach¹⁰⁵, M Ouchrif^{135d}, F Ould-Saada¹¹⁷, A Ouraou¹³⁶, Q Ouyang^{32a}, M Owen⁸², S Owen¹³⁹, A Oyarzun^{31b}, O K Øye¹³, V E Ozcan^{18a}, N Ozturk⁷, A Pacheco Pages¹¹, C Padilla Aranda¹¹, E Paganis¹³⁹, F Paige²⁴, K Pajchel¹¹⁷, S Palestini²⁹, D Pallin³³, A Palma^{124a,179}, J D Palmer¹⁷, Y B Pan¹⁷², E Panagiotopoulou⁹, B Panes^{31a}, N Panikashvili⁸⁷, S Panitkin²⁴, D Pantea^{25a}, M Panuskova¹²⁵, V Paolone¹²³, A Paoloni^{133a,133b}, A Papadelis^{146a}, Th D Papadopoulou⁹, A Paramonov⁵, W Park^{24,199}, M A Parker²⁷, F Parodi^{50a,50b}, J A Parsons³⁴, U Parzefall⁴⁸, E Pasqualucci^{132a}, A Passeri^{134a}, F Pastore^{134a,134b}, Fr Pastore²⁹, G Pásztor^{49,200}, S Pataraja¹⁷², N Patel¹⁵⁰, J R Pater⁸², S Patricelli^{102a,102b}, T Pauly²⁹, M Pecsny^{144a}, M I Pedraza Morales¹⁷², S V Peleganchuk¹⁰⁷, H Peng¹⁷², R Pengo²⁹, A Penson³⁴, J Penwell⁶¹, M Perantoni^{23a}, K Perez^{34,195}, T Perez Cavalcanti⁴¹, E Perez Codina¹¹, M T Pérez García-Estañ¹⁶⁷, V Perez Reale³⁴, I Peric²⁰, L Perini^{89a,89b}, H Pernegger²⁹, R Perrino^{72a}, P Perrodo⁴, S Persebe^{3a}, V D Peshekhonov⁶⁵, O Peters¹⁰⁵, B A Petersen²⁹, J Petersen²⁹, T C Petersen³⁵, E Petit⁸³, A Petridis¹⁵⁴, C Petridou¹⁵⁴, E Petrolo^{132a}, F Petrucci^{134a,134b}, D Petschull⁴¹, M Petteni¹⁴², R Pezoa^{31b}, A Phan⁸⁶, A W Phillips²⁷, P W Phillips¹²⁹, G Piacquadio²⁹, E Piccaro⁷⁵, M Piccinini^{19a,19b}, A Pickford⁵³, S M Picc⁴¹, R Piegai²⁶, J E Pilcher³⁰, A D Pilkington⁸², J Pina^{124a,179}, M Pinamonti^{164a,164c}, A Pinder¹¹⁸, J L Pinfold², J Ping^{32c}, B Pinto^{124a,179}, O Pirotte²⁹, C Pizio^{89a,89b}, R Placakyte⁴¹, M Plamondon¹⁶⁹, W G Plano⁸², M-A Pleier²⁴, A V Pleskach¹²⁸, A Poblaguev²⁴, S Poddar^{58a}, F Podlyski³³, L Poggioli¹¹⁵, T Poghosyan²⁰, M Pohl⁴⁹, F Polci⁵⁵, G Polesello^{119a}, A Policicchio¹³⁸, A Polini^{19a}, J Poll⁷⁵, V Polychronakos²⁴, D M Pomarede¹³⁶, D Pomeroy²², K Pommès²⁹, L Pontecorvo^{132a}, B G Pope⁸⁸, G A Popeneciu^{25a}, D S Popovic^{12a}, A Poppleton²⁹, X Portell Bueso⁴⁸, R Porter¹⁶³, C Posch²¹, G E Pospelov⁹⁹, S Pospisil¹²⁷, I N Potrap⁹⁹, C J Potter¹⁴⁹, C T Potter¹¹⁴, G Poulard²⁹, J Poveda¹⁷², R Prabhu⁷⁷, P Pralavorio⁸³, S Prasad⁵⁷, R Pravahan⁷, S Prell⁶⁴, K Pretzl¹⁶, L Pribyl²⁹, D Price⁶¹, L E Price⁵, M J Price²⁹, P M Prichard⁷³, D Prieur¹²³, M Primavera^{72a}, K Prokofiev¹⁰⁸, F Prokoshin^{31b}, S Protopopescu²⁴, J Proudfoot⁵, X Prudent⁴³, H Przysiechniak⁴, S Psoroulas²⁰, E Ptacek¹¹⁴, J Purdham⁸⁷, M Purohit^{24,199}, P Puzo¹¹⁵, Y Pylypchenko¹¹⁷, J Qian⁸⁷, Z Qian⁸³, Z Qin⁴¹, A Quadt⁵⁴, D R Quarrie¹⁴, W B Quayle¹⁷², F Quinonez^{31a}, M Raas¹⁰⁴, V Radescu^{58b}, B Radics²⁰, T Rador^{18a}, F Ragusa^{89a,89b}, G Rahal¹⁷⁷, A M Rahimi¹⁰⁹, D Rahm²⁴, S Rajagopalan²⁴, S Rajek⁴², M Rammensee⁴⁸,

M Rammes¹⁴¹, M Ramstedt^{146a,146b}, K Randrianarivony²⁸, P N Ratoff⁷¹, F Rauscher⁹⁸, E Rauter⁹⁹, M Raymond²⁹, A L Read¹¹⁷, D M Rebuffi^{119a,119b}, A Redelbach¹⁷³, G Redlinger²⁴, R Reece¹²⁰, K Reeves⁴⁰, A Reichold¹⁰⁵, E Reinherz-Aronis¹⁵³, A Reinsch¹¹⁴, I Reisinger⁴², D Reljic^{12a}, C Rembser²⁹, Z L Ren¹⁵¹, A Renaud¹¹⁵, P Renkel³⁹, B Rensch³⁵, M Rescigno^{132a}, S Resconi^{89a}, B Resende¹³⁶, P Reznicek⁹⁸, R Rezvani¹⁵⁸, A Richards⁷⁷, R Richter⁹⁹, E Richter-Was^{38,201}, M Ridel⁷⁸, S Rieke⁸¹, M Rijpstra¹⁰⁵, M Rijssenbeek¹⁴⁸, A Rimoldi^{119a,119b}, L Rinaldi^{19a}, R Rios³⁹, I Riu¹¹, G Rivoltella^{89a,89b}, F Rizatdinova¹¹², E Rizvi⁷⁵, S H Robertson^{85,186}, A Robichaud-Veronneau⁴⁹, D Robinson²⁷, J E M Robinson⁷⁷, M Robinson¹¹⁴, A Robson⁵³, J G Rocha de Lima¹⁰⁶, C Roda^{122a,122b}, D Roda Dos Santos²⁹, S Rodier⁸⁰, D Rodriguez¹⁶², Y Rodriguez Garcia¹⁵, A Roe⁵⁴, S Roe²⁹, O Røhne¹¹⁷, V Rojo¹, S Rolli¹⁶¹, A Romaniouk⁹⁶, V M Romanov⁶⁵, G Romeo²⁶, D Romero Maltrana^{31a}, L Roos⁷⁸, E Ros¹⁶⁷, S Rosati^{132a,132b}, M Rose⁷⁶, G A Rosenbaum¹⁵⁸, E I Rosenberg⁶⁴, P L Rosendahl¹³, L Rossetet⁴⁹, V Rossetti¹¹, E Rossi^{102a,102b}, L P Rossi^{50a}, L Rossi^{89a,89b}, M Rotaru^{25a}, I Roth¹⁷¹, J Rothberg¹³⁸, I Rottländer²⁰, D Rousseau¹¹⁵, C R Royon¹³⁶, A Rozanov⁸³, Y Rozen¹⁵², X Ruan¹¹⁵, I Rubinskiy⁴¹, B Ruckert⁹⁸, N Ruckstuhl¹⁰⁵, V I Rud⁹⁷, G Rudolph⁶², F Rühr⁶, F Ruggieri^{134a,134b}, A Ruiz-Martinez⁶⁴, E Rulikowska-Zarebska³⁷, V Rumiantsev^{91,206}, L Rummyantsev⁶⁵, K Runge⁴⁸, O Runolfsson²⁰, Z Rurikova⁴⁸, N A Rusakovich⁶⁵, D R Rust⁶¹, J P Rutherford⁶, C Ruwiedel¹⁴, P Ruzicka¹²⁵, Y F Ryabov¹²¹, V Ryadovikov¹²⁸, P Ryan⁸⁸, M Rybar¹²⁶, G Rybkin¹¹⁵, N C Ryder¹¹⁸, S Rzaeva¹⁰, A F Saavedra¹⁵⁰, I Sadeh¹⁵³, H F-W Sadrozinski¹³⁷, R Sadykov⁶⁵, F Safai Tehrani^{132a,132b}, H Sakamoto¹⁵⁵, G Salamanna¹⁰⁵, A Salamon^{133a}, M Saleem¹¹¹, D Salihagic⁹⁹, A Salnikov¹⁴³, J Salt¹⁶⁷, B M Salvachua Ferrando⁵, D Salvatore^{36a,36b}, F Salvatore¹⁴⁹, A Salzburger²⁹, D Sampsonidis¹⁵⁴, B H Samset¹¹⁷, H Sandaker¹³, H G Sander⁸¹, M P Sanders⁹⁸, M Sandhoff¹⁷⁴, P Sandhu¹⁵⁸, T Sandoval²⁷, R Sandstroem¹⁰⁵, S Sandvoss¹⁷⁴, D P C Sankey¹²⁹, A Sansoni⁴⁷, C Santamarina Rios⁸⁵, C Santoni³³, R Santonico^{133a,133b}, H Santos^{124a}, J G Saraiva^{124a,179}, T Sarangi¹⁷², E Sarkisyan-Grinbaum⁷, F Sarri^{122a,122b}, G Sartisohn¹⁷⁴, O Sasaki⁶⁶, T Sasaki⁶⁶, N Sasao⁶⁸, I Satsounkevitch⁹⁰, G Sauvage⁴, J B Sauvan¹¹⁵, P Savard^{158,181}, V Savinov¹²³, D O Savu²⁹, P Savva⁹, L Sawyer^{24,187}, D H Saxon⁵³, L P Says³³, C Sbarra^{19a,19b}, A Sbrizzi^{19a,19b}, O Scallon⁹³, D A Scannicchio¹⁶³, J Schaarschmidt¹¹⁵, P Schacht⁹⁹, U Schäfer⁸¹, S Schaepe²⁰, S Schaezel^{58b}, A C Schaffer¹¹⁵, D Schaile⁹⁸, R D Schamberger¹⁴⁸, A G Schamov¹⁰⁷, V Scharf^{58a}, V A Schegelsky¹²¹, D Scheirich⁸⁷, M I Scherzer¹⁴, C Schiavi^{50a,50b}, J Schieck⁹⁸, M Schioppa^{36a,36b}, S Schlenker²⁹, J L Schlereth⁵, E Schmidt⁴⁸, M P Schmidt^{175,206}, K Schmieden²⁰, C Schmitt⁸¹, M Schmitz²⁰, A Schöning^{58b}, M Schott²⁹, D Schouten¹⁴², J Schovancova¹²⁵, M Schram⁸⁵, C Schroeder⁸¹, N Schroer^{58c}, S Schuh²⁹, G Schuler²⁹, J Schultes¹⁷⁴, H-C Schultz-Coulon^{58a}, H Schulz¹⁵, J W Schumacher²⁰, M Schumacher⁴⁸, B A Schumm¹³⁷, Ph Schune¹³⁶, C Schwanenberger⁸², A Schwartzman¹⁴³, Ph Schwemling⁷⁸, R Schwienhorst⁸⁸, R Schwierz⁴³, J Schwindling¹³⁶, W G Scott¹²⁹, J Searcy¹¹⁴, E Sedykh¹²¹, E Segura¹¹, S C Seidel¹⁰³, A Seiden¹³⁷, F Seifert⁴³, J M Seixas^{23a}, G Sekhniaidze^{102a}, D M Seliverstov¹²¹, B Sellden^{146a}, G Sellers⁷³, M Seman^{144b}, N Semprini-Cesari^{19a,19b}, C Serfon⁹⁸, L Serin¹¹⁵, R Seuster⁹⁹, H Severini¹¹¹, M E Sevir⁸⁶, A Sfyrła²⁹, E Shabalina⁵⁴, M Shamim¹¹⁴, L Y Shan^{32a}, J T Shank²¹, Q T Shao⁸⁶, M Shapiro¹⁴, P B Shatalov⁹⁵, L Shaver⁶, C Shaw⁵³, K Shaw^{164a,164c}, D Sherman¹⁷⁵, P Sherwood⁷⁷, A Shibata¹⁰⁸, S Shimizu²⁹, M Shimojima¹⁰⁰, T Shin⁵⁶, A Shmeleva⁹⁴, M J Shochet³⁰, D Short¹¹⁸, M A Shupe⁶, P Sicho¹²⁵, A Sidoti^{132a,132b}, A Siebel¹⁷⁴, F Siegert⁴⁸, J Siegrist¹⁴, Dj Sijacki^{12a}, O Silbert¹⁷¹, J Silva^{124a,179}, Y Silver¹⁵³, D Silverstein¹⁴³, S B Silverstein^{146a}, V Simak¹²⁷, O Simard¹³⁶, Lj Simic^{12a}, S Simion¹¹⁵, B Simmons⁷⁷, M Simonyan³⁵, P Sinervo¹⁵⁸, N B Sinev¹¹⁴, V Sipica¹⁴¹, G Siragusa⁸¹, A N Sisakyan⁶⁵, S Yu Sivoklov⁹⁷, J Sjölin^{146a,146b}, T B Sjusen¹³, L A Skinnari¹⁴,

K Skovpen¹⁰⁷, P Skubic¹¹¹, N Skvorodnev²², M Slater¹⁷, T Slavicek¹²⁷, K Sliwa¹⁶¹, T J Sloan⁷¹, J Sloper²⁹, V Smakhtin¹⁷¹, S Yu Smirnov⁹⁶, L N Smirnova⁹⁷, O Smirnova⁷⁹, B C Smith⁵⁷, D Smith¹⁴³, K M Smith⁵³, M Smizanska⁷¹, K Smolek¹²⁷, A A Snesev⁹⁴, S W Snow⁸², J Snow¹¹¹, J Snuverink¹⁰⁵, S Snyder²⁴, M Soares^{124a}, R Sobie^{169,186}, J Sodomka¹²⁷, A Soffer¹⁵³, C A Solans¹⁶⁷, M Solar¹²⁷, J Solc¹²⁷, E Soldatov⁹⁶, U Soldevila¹⁶⁷, E Solfaroli Camillocci^{132a,132b}, A A Solodkov¹²⁸, O V Solovyanov¹²⁸, J Sondericker²⁴, N Soni², V Sopko¹²⁷, B Sopko¹²⁷, M Sorbi^{89a,89b}, M Sosebee⁷, A Soukharev¹⁰⁷, S Spagnolo^{72a,72b}, F Spanò³⁴, R Spighi^{19a}, G Spigo²⁹, F Spila^{132a,132b}, E Spiriti^{134a}, R Spiwojs²⁹, M Spousta¹²⁶, T Spreitzer¹⁵⁸, B Spurlock⁷, R D St Denis⁵³, T Stahl¹⁴¹, J Stahlman¹²⁰, R Stamen^{58a}, E Stanecka²⁹, R W Stanek⁵, C Stanescu^{134a}, S Stapnes¹¹⁷, E A Starchenko¹²⁸, J Stark⁵⁵, P Staroba¹²⁵, P Starovoitov⁹¹, A Staude⁹⁸, P Stavina^{144a}, G Stavropoulos¹⁴, G Steele⁵³, P Steinbach⁴³, P Steinberg²⁴, I Stekl¹²⁷, B Stelzer¹⁴², H J Stelzer⁴¹, O Stelzer-Chilton^{159a}, H Stenzel⁵², K Stevenson⁷⁵, G A Stewart⁵³, J A Stillings²⁰, T Stockmanns²⁰, M C Stockton²⁹, K Stoerig⁴⁸, G Stoicea^{25a}, S Stonjek⁹⁹, P Strachota¹²⁶, A R Stradling⁷, A Straessner⁴³, J Strandberg⁸⁷, S Strandberg^{146a,146b}, A Strandlie¹¹⁷, M Strang¹⁰⁹, E Strauss¹⁴³, M Strauss¹¹¹, P Strizenec^{144b}, R Ströhmer¹⁷³, D M Strom¹¹⁴, J A Strong^{76,206}, R Stroynowski³⁹, J Strube¹²⁹, B Stugu¹³, I Stumer^{24,206}, J Stupak¹⁴⁸, P Sturm¹⁷⁴, D A Soh^{151,192}, D Su¹⁴³, HS Subramania², Y Sugaya¹¹⁶, T Sugimoto¹⁰¹, C Suhr¹⁰⁶, K Suita⁶⁷, M Suk¹²⁶, V V Sulin⁹⁴, S Sultansoy^{3d}, T Sumida²⁹, X Sun⁵⁵, J E Sundermann⁴⁸, K Suruliz^{164a,164b}, S Sushkov¹¹, G Susinno^{36a,36b}, M R Sutton¹³⁹, Y Suzuki⁶⁶, Yu M Sviridov¹²⁸, S Swedish¹⁶⁸, I Sykora^{144a}, T Sykora¹²⁶, B Szeless²⁹, J Sánchez¹⁶⁷, D Ta¹⁰⁵, K Tackmann²⁹, A Taffard¹⁶³, R Tafirout^{159a}, A Taga¹¹⁷, N Taiblum¹⁵³, Y Takahashi¹⁰¹, H Takai²⁴, R Takashima⁶⁹, H Takeda⁶⁷, T Takeshita¹⁴⁰, M Talby⁸³, A Talyshev¹⁰⁷, M C Tamsett²⁴, J Tanaka¹⁵⁵, R Tanaka¹¹⁵, S Tanaka¹³¹, S Tanaka⁶⁶, Y Tanaka¹⁰⁰, K Tani⁶⁷, N Tannoury⁸³, G P Tappern²⁹, S Tapprogge⁸¹, D Tardif¹⁵⁸, S Tarem¹⁵², F Tarrade²⁴, G F Tartarelli^{89a}, P Tas¹²⁶, M Tasevsky¹²⁵, E Tassi^{36a,36b}, M Tatarkhanov¹⁴, C Taylor⁷⁷, F E Taylor⁹², G N Taylor⁸⁶, W Taylor^{159b}, M Teixeira Dias Castanheira⁷⁵, P Teixeira-Dias⁷⁶, K K Temming⁴⁸, H Ten Kate²⁹, P K Teng¹⁵¹, S Terada⁶⁶, K Terashi¹⁵⁵, J Terron⁸⁰, M Terwort^{41,190}, M Testa⁴⁷, R J Teuscher^{158,186}, C M Tevlin⁸², J Thadome¹⁷⁴, J Therhaag²⁰, T Theveneaux-Pelzer⁷⁸, M Thioye¹⁷⁵, S Thoma⁴⁸, J P Thomas¹⁷, E N Thompson⁸⁴, P D Thompson¹⁷, P D Thompson¹⁵⁸, A S Thompson⁵³, E Thomson¹²⁰, M Thomson²⁷, R P Thun⁸⁷, T Tic¹²⁵, V O Tikhomirov⁹⁴, Y A Tikhonov¹⁰⁷, C J W P Timmermans¹⁰⁴, P Tipton¹⁷⁵, F J Tique Aires Viegas²⁹, S Tisserant⁸³, J Tobias⁴⁸, B Toczec³⁷, T Todorov⁴, S Todorova-Nova¹⁶¹, B Toggerson¹⁶³, J Tojo⁶⁶, S Tokár^{144a}, K Tokunaga⁶⁷, K Tokushuku⁶⁶, K Tollefsen⁸⁸, M Tomoto¹⁰¹, L Tompkins¹⁴, K Toms¹⁰³, A Tonazzo^{134a,134b}, G Tong^{32a}, A Tonoyan¹³, C Topfel¹⁶, N D Topilin⁶⁵, I Torchiani²⁹, E Torrence¹¹⁴, E Torró Pastor¹⁶⁷, J Toth^{83,200}, F Touchard⁸³, D R Tovey¹³⁹, D Traynor⁷⁵, T Trefzger¹⁷³, J Treis²⁰, L Tremblet²⁹, A Tricoli²⁹, I M Trigger^{159a}, S Trincas-Duvoid⁷⁸, T N Trinh⁷⁸, M F Tripiana⁷⁰, N Triplett⁶⁴, W Trischuk¹⁵⁸, A Trivedi^{24,199}, B Trocmé⁵⁵, C Troncon^{89a}, M Trottier-McDonald¹⁴², A Trzupek³⁸, C Tsarouchas²⁹, J C-L Tseng¹¹⁸, M Tsiakiris¹⁰⁵, P V Tsiareshka⁹⁰, D Tsionou⁴, G Tsiopolitis⁹, V Tsiskaridze⁴⁸, E G Tskhadadze⁵¹, I I Tsukerman⁹⁵, V Tsulaia¹²³, J-W Tsung²⁰, S Tsuno⁶⁶, D Tsybychev¹⁴⁸, A Tua¹³⁹, J M Tuggle³⁰, M Turala³⁸, D Turecek¹²⁷, I Turk Cakir^{3e}, E Turlay¹⁰⁵, R Turra^{89a,89b}, P M Tuts³⁴, A Tykhonov⁷⁴, M Tylmad^{146a,146b}, M Tyndel¹²⁹, D Typaldos¹⁷, H Tyrvaainen²⁹, G Tzanakos⁸, K Uchida²⁰, I Ueda¹⁵⁵, R Ueno²⁸, M Ugland¹³, M Uhlenbrock²⁰, M Uhrmacher⁵⁴, F Ukegawa¹⁶⁰, G Unal²⁹, D G Underwood⁵, A Undrus²⁴, G Unel¹⁶³, Y Unno⁶⁶, D Urbaniec³⁴, E Urkovsky¹⁵³, P Urquijo⁴⁹, P Urrejola^{31a}, G Usai⁷, M Uslenghi^{119a,119b}, L Vacavant⁸³, V Vacek¹²⁷, B Vachon⁸⁵, S Vahsen¹⁴, C Valderanis⁹⁹, J Valenta¹²⁵, P Valente^{132a}, S Valentinetti^{19a,19b}, S Valkar¹²⁶, E Valladolid Gallego¹⁶⁷, S Vallecorsa¹⁵², J A Valls Ferrer¹⁶⁷, H van der Graaf¹⁰⁵, E van der Kraaij¹⁰⁵,

R Van Der Leeuw¹⁰⁵, E van der Poel¹⁰⁵, D van der Ster²⁹, B Van Eijk¹⁰⁵, N van Eldik⁸⁴, P van Gemmeren⁵, Z van Kesteren¹⁰⁵, I van Vulpen¹⁰⁵, W Vandelli²⁹, G Vandoni²⁹, A Vaniachine⁵, P Vankov⁴¹, F Vannucci⁷⁸, F Varela Rodriguez²⁹, R Vari^{132a}, E W Varnes⁶, D Varouchas¹⁴, A Vartapetian⁷, K E Varvell¹⁵⁰, V I Vassilakopoulos⁵⁶, F Vazeille³³, G Vegni^{89a,89b}, J J Veillet¹¹⁵, C Vellidis⁸, F Veloso^{124a}, R Veness²⁹, S Veneziano^{132a}, A Ventura^{72a,72b}, D Ventura¹³⁸, M Venturi⁴⁸, N Venturi¹⁶, V Vercesi^{119a}, M Verducci¹³⁸, W Verkerke¹⁰⁵, J C Vermeulen¹⁰⁵, A Vest⁴³, M C Vetterli^{142,181}, I Vichou¹⁶⁵, T Vickey^{145b,202}, G H A Viehhauser¹¹⁸, S Viel¹⁶⁸, M Villa^{19a,19b}, M Villaplana Perez¹⁶⁷, E Vilucchi⁴⁷, M G Vinciter²⁸, E Vinek²⁹, V B Vinogradov⁶⁵, M Virchaux^{136,206}, S Viret³³, J Virzi¹⁴, A Vitale^{19a,19b}, O Vitells¹⁷¹, M Viti⁴¹, I Vivarelli⁴⁸, F Vives Vaque¹¹, S Vlachos⁹, M Vlasak¹²⁷, N Vlasov²⁰, A Vogel²⁰, P Vokac¹²⁷, G Volpi⁴⁷, M Volpi¹¹, G Volpini^{89a}, H von der Schmitt⁹⁹, J von Loeben⁹⁹, H von Radziewski⁴⁸, E von Toerne²⁰, V Vorobel¹²⁶, A P Vorobiev¹²⁸, V Vorwerk¹¹, M Vos¹⁶⁷, R Voss²⁹, T T Voss¹⁷⁴, J H Vosseveld⁷³, A S Vovenko¹²⁸, N Vranjes^{12a}, M Vranjes Milosavljevic^{12a}, V Vrba¹²⁵, M Vreeswijk¹⁰⁵, T Vu Anh⁸¹, R Vuillermet²⁹, I Vukotic¹¹⁵, W Wagner¹⁷⁴, P Wagner¹²⁰, H Wahlen¹⁷⁴, J Wakabayashi¹⁰¹, J Walbersloh⁴², S Walch⁸⁷, J Walder⁷¹, R Walker⁹⁸, W Walkowiak¹⁴¹, R Wall¹⁷⁵, P Waller⁷³, C Wang⁴⁴, H Wang¹⁷², J Wang¹⁵¹, J Wang^{32d}, J C Wang¹³⁸, R Wang¹⁰³, S M Wang¹⁵¹, A Warburton⁸⁵, C P Ward²⁷, M Warsinsky⁴⁸, P M Watkins¹⁷, A T Watson¹⁷, M F Watson¹⁷, G Watts¹³⁸, S Watts⁸², A T Waugh¹⁵⁰, B M Waugh⁷⁷, J Weber⁴², M Weber¹²⁹, M S Weber¹⁶, P Weber⁵⁴, A R Weidberg¹¹⁸, P Weigell⁹⁹, J Weingarten⁵⁴, C Weiser⁴⁸, H Wellenstein²², P S Wells²⁹, M Wen⁴⁷, T Wenaus²⁴, S Wendler¹²³, Z Weng^{151,192}, T Wengler²⁹, S Wenig²⁹, N Wermes²⁰, M Werner⁴⁸, P Werner²⁹, M Werth¹⁶³, M Wessels^{58a}, K Whalen²⁸, S J Wheeler-Ellis¹⁶³, S P Whitaker²¹, A White⁷, M J White⁸⁶, S White²⁴, S R Whitehead¹¹⁸, D Whiteson¹⁶³, D Whittington⁶¹, F Wicek¹¹⁵, D Wicke¹⁷⁴, F J Wickens¹²⁹, W Wiedenmann¹⁷², M Wielers¹²⁹, P Wienemann²⁰, C Wiglesworth⁷³, L A M Wiik⁴⁸, P A Wijeratne⁷⁷, A Wildauer¹⁶⁷, M A Wildt^{41,190}, I Wilhelm¹²⁶, H G Wilkens²⁹, J Z Will⁹⁸, E Williams³⁴, H H Williams¹²⁰, W Willis³⁴, S Willocq⁸⁴, J A Wilson¹⁷, M G Wilson¹⁴³, A Wilson⁸⁷, I Wingerter-Seez⁴, S Winkelmann⁴⁸, F Winklmeier²⁹, M Wittgen¹⁴³, M W Wolter³⁸, H Wolters^{124a,184}, G Wooden¹¹⁸, B K Wosiek³⁸, J Wotschack²⁹, M J Woudstra⁸⁴, K Wraight⁵³, C Wright⁵³, B Wrona⁷³, S L Wu¹⁷², X Wu⁴⁹, Y Wu^{32b}, E Wulf³⁴, R Wunstorff⁴², B M Wynne⁴⁵, L Xaplanteris⁹, S Xella³⁵, S Xie⁴⁸, Y Xie^{32a}, C Xu^{32b}, D Xu¹³⁹, G Xu^{32a}, B Yabsley¹⁵⁰, M Yamada⁶⁶, A Yamamoto⁶⁶, K Yamamoto⁶⁴, S Yamamoto¹⁵⁵, T Yamamura¹⁵⁵, J Yamaoka⁴⁴, T Yamazaki¹⁵⁵, Y Yamazaki⁶⁷, Z Yan²¹, H Yang⁸⁷, U K Yang⁸², Y Yang⁶¹, Y Yang^{32a}, Z Yang^{146a,146b}, S Yanush⁹¹, W-M Yao¹⁴, Y Yao¹⁴, Y Yasu⁶⁶, G V Ybeles Smit¹³⁰, J Ye³⁹, S Ye²⁴, M Yilmaz^{3c}, R Yoosoofmiya¹²³, K Yorita¹⁷⁰, R Yoshida⁵, C Young¹⁴³, S Youssef²¹, D Yu²⁴, J Yu⁷, J Yu^{32c,203}, L Yuan^{32a,204}, A Yurkewicz¹⁴⁸, V G Zaets¹²⁸, R Zaidan⁶³, A M Zaitsev¹²⁸, Z Zajacova²⁹, Yo K Zalite¹²¹, L Zanello^{132a,132b}, P Zarzhitsky³⁹, A Zaytsev¹⁰⁷, C Zeitnitz¹⁷⁴, M Zeller¹⁷⁵, P F Zema²⁹, A Zemla³⁸, C Zendler²⁰, A V Zenin¹²⁸, O Zenin¹²⁸, T Ženiš^{144a}, Z Zenonos^{122a,122b}, S Zenz¹⁴, D Zerwas¹¹⁵, A Zerwekh^{31b}, G Zevi della Porta⁵⁷, Z Zhan^{32d}, D Zhang^{32b}, H Zhang⁸⁸, J Zhang⁵, X Zhang^{32d}, Z Zhang¹¹⁵, L Zhao¹⁰⁸, T Zhao¹³⁸, Z Zhao^{32b}, A Zhemchugov⁶⁵, S Zheng^{32a}, J Zhong^{151,205}, B Zhou⁸⁷, N Zhou¹⁶³, Y Zhou¹⁵¹, C G Zhu^{32d}, H Zhu⁴¹, Y Zhu¹⁷², X Zhuang⁹⁸, V Zhuravlov⁹⁹, D Zieminska⁶¹, B Zilka^{144a}, R Zimmermann²⁰, S Zimmermann²⁰, S Zimmermann⁴⁸, M Ziolkowski¹⁴¹, R Zitoun⁴, L Živković³⁴, V V Zmouchko^{128,206}, G Zobernig¹⁷², A Zoccoli^{19a,19b}, Y Zolnierowski⁴, A Zsenci²⁹, M zur Nedden¹⁵, V Zutshi¹⁰⁶ and L Zwalinski²⁹

¹ University at Albany, Albany NY, USA

² Department of Physics, University of Alberta, Edmonton AB, Canada

^{3a} Department of Physics, Ankara University, Ankara, Turkey

- ^{3b} Department of Physics, Dumlupinar University, Kutahya, Turkey
- ^{3c} Department of Physics, Gazi University, Ankara, Turkey
- ^{3d} Division of Physics, TOBB University of Economics and Technology, Ankara, Turkey
- ^{3e} Turkish Atomic Energy Authority, Ankara, Turkey
- ⁴ LAPP, CNRS/IN2P3 and Université de Savoie, Annecy-le-Vieux, France
- ⁵ High Energy Physics Division, Argonne National Laboratory, Argonne IL, USA
- ⁶ Department of Physics, University of Arizona, Tucson AZ, USA
- ⁷ Department of Physics, The University of Texas at Arlington, Arlington TX, USA
- ⁸ Physics Department, University of Athens, Athens, Greece
- ⁹ Physics Department, National Technical University of Athens, Zografou, Greece
- ¹⁰ Institute of Physics, Azerbaijan Academy of Sciences, Baku, Azerbaijan
- ¹¹ Institut de Física d'Altes Energies and Universitat Autònoma de Barcelona and ICREA, Barcelona, Spain
- ^{12a} Institute of Physics, University of Belgrade, Belgrade, Serbia
- ^{12b} Vinca Institute of Nuclear Sciences, Belgrade, Serbia
- ¹³ Department for Physics and Technology, University of Bergen, Bergen, Norway
- ¹⁴ Physics Division, Lawrence Berkeley National Laboratory and University of California, Berkeley CA, USA
- ¹⁵ Department of Physics, Humboldt University, Berlin, Germany
- ¹⁶ Albert Einstein Center for Fundamental Physics and Laboratory for High Energy Physics, University of Bern, Bern, Switzerland
- ¹⁷ School of Physics and Astronomy, University of Birmingham, Birmingham, United Kingdom
- ^{18a} Department of Physics, Bogazici University, Istanbul, Turkey
- ^{18b} Division of Physics, Dogus University, Istanbul, Turkey
- ^{18c} Department of Physics Engineering, Gaziantep University, Gaziantep, Turkey
- ^{18d} Department of Physics, Istanbul Technical University, Istanbul, Turkey
- ^{19a} INFN Sezione di Bologna, Bologna, Italy
- ^{19b} Dipartimento di Fisica, Università di Bologna, Bologna, Italy
- ²⁰ Physikalisches Institut, University of Bonn, Bonn, Germany
- ²¹ Department of Physics, Boston University, Boston MA, USA
- ²² Department of Physics, Brandeis University, Waltham MA, USA
- ^{23a} Universidade Federal do Rio De Janeiro COPPE/EE/IF, Rio de Janeiro, Brazil
- ^{23b} Instituto de Física, Universidade de Sao Paulo, Sao Paulo, Brazil
- ²⁴ Physics Department, Brookhaven National Laboratory, Upton NY, USA
- ^{25a} National Institute of Physics and Nuclear Engineering, Bucharest, Romania
- ^{25b} University Politehnica Bucharest, Bucharest, Romania
- ^{25c} West University in Timisoara, Timisoara, Romania
- ²⁶ Departamento de Física, Universidad de Buenos Aires, Buenos Aires, Argentina
- ²⁷ Cavendish Laboratory, University of Cambridge, Cambridge, United Kingdom
- ²⁸ Department of Physics, Carleton University, Ottawa ON, Canada
- ²⁹ CERN, Geneva, Switzerland
- ³⁰ Enrico Fermi Institute, University of Chicago, Chicago IL, USA
- ^{31a} Departamento de Física, Pontificia Universidad Católica de Chile, Santiago, Chile
- ^{31b} Departamento de Física, Universidad Técnica Federico Santa María, Valparaíso, Chile

- ^{32a} Institute of High Energy Physics, Chinese Academy of Sciences, Beijing, China
- ^{32b} Department of Modern Physics, University of Science and Technology of China, Anhui, China
- ^{32c} Department of Physics, Nanjing University, Jiangsu, China
- ^{32d} High Energy Physics Group, Shandong University, Shandong, China
- ³³ Laboratoire de Physique Corpusculaire, Clermont Université and Université Blaise Pascal and CNRS/IN2P3, Aubiere Cedex, France
- ³⁴ Nevis Laboratory, Columbia University, Irvington NY, USA
- ³⁵ Niels Bohr Institute, University of Copenhagen, Kobenhavn, Denmark
- ^{36a} INFN Gruppo Collegato di Cosenza, Italy
- ^{36b} Dipartimento di Fisica, Università della Calabria, Arcavata di Rende, Italy
- ³⁷ Faculty of Physics and Applied Computer Science, AGH-University of Science and Technology, Krakow, Poland
- ³⁸ The Henryk Niewodniczanski Institute of Nuclear Physics, Polish Academy of Sciences, Krakow, Poland
- ³⁹ Physics Department, Southern Methodist University, Dallas TX, USA
- ⁴⁰ Physics Department, University of Texas at Dallas, Richardson TX, USA
- ⁴¹ DESY, Hamburg and Zeuthen, Germany
- ⁴² Institut für Experimentelle Physik IV, Technische Universität Dortmund, Dortmund, Germany
- ⁴³ Institut für Kern- und Teilchenphysik, Technical University Dresden, Dresden, Germany
- ⁴⁴ Department of Physics, Duke University, Durham NC, USA
- ⁴⁵ SUPA—School of Physics and Astronomy, University of Edinburgh, Edinburgh, United Kingdom
- ⁴⁶ Fachhochschule Wiener Neustadt, Wiener Neustadt, Austria
- ⁴⁷ INFN Laboratori Nazionali di Frascati, Frascati, Italy
- ⁴⁸ Fakultät für Mathematik und Physik, Albert-Ludwigs-Universität, Freiburg i.Br., Germany
- ⁴⁹ Section de Physique, Université de Genève, Geneva, Switzerland
- ^{50a} INFN Sezione di Genova, Genova, Italy
- ^{50b} Dipartimento di Fisica, Università di Genova, Genova, Italy
- ⁵¹ Institute of Physics and HEP Institute, Georgian Academy of Sciences and Tbilisi State University, Tbilisi, Georgia
- ⁵² II Physikalisches Institut, Justus-Liebig-Universität Giessen, Giessen, Germany
- ⁵³ SUPA—School of Physics and Astronomy, University of Glasgow, Glasgow, United Kingdom
- ⁵⁴ II Physikalisches Institut, Georg-August-Universität, Göttingen, Germany
- ⁵⁵ Laboratoire de Physique Subatomique et de Cosmologie, Université Joseph Fourier and CNRS/IN2P3 and Institut National Polytechnique de Grenoble, Grenoble, France
- ⁵⁶ Department of Physics, Hampton University, Hampton VA, USA
- ⁵⁷ Laboratory for Particle Physics and Cosmology, Harvard University, Cambridge MA, USA
- ^{58a} Kirchhoff-Institut für Physik, Ruprecht-Karls-Universität Heidelberg, Heidelberg, Germany
- ^{58b} Physikalisches Institut, Ruprecht-Karls-Universität Heidelberg, Heidelberg, Germany
- ^{58c} ZITI Institut für technische Informatik, Ruprecht-Karls-Universität Heidelberg, Mannheim, Germany

- ⁵⁹ Faculty of Science, Hiroshima University, Hiroshima, Japan
- ⁶⁰ Faculty of Applied Information Science, Hiroshima Institute of Technology, Hiroshima, Japan
- ⁶¹ Department of Physics, Indiana University, Bloomington IN, USA
- ⁶² Institut für Astro- und Teilchenphysik, Leopold-Franzens-Universität, Innsbruck, Austria
- ⁶³ University of Iowa, Iowa City IA, USA
- ⁶⁴ Department of Physics and Astronomy, Iowa State University, Ames IA, USA
- ⁶⁵ Joint Institute for Nuclear Research, JINR Dubna, Dubna, Russia
- ⁶⁶ KEK, High Energy Accelerator Research Organization, Tsukuba, Japan
- ⁶⁷ Graduate School of Science, Kobe University, Kobe, Japan
- ⁶⁸ Faculty of Science, Kyoto University, Kyoto, Japan
- ⁶⁹ Kyoto University of Education, Kyoto, Japan
- ⁷⁰ Instituto de Física La Plata, Universidad Nacional de La Plata and CONICET, La Plata, Argentina
- ⁷¹ Physics Department, Lancaster University, Lancaster, United Kingdom
- ^{72a} INFN Sezione di Lecce, Lecce, Italy
- ^{72b} Dipartimento di Fisica, Università del Salento, Lecce, Italy
- ⁷³ Oliver Lodge Laboratory, University of Liverpool, Liverpool, United Kingdom
- ⁷⁴ Department of Physics, Jožef Stefan Institute and University of Ljubljana, Ljubljana, Slovenia
- ⁷⁵ Department of Physics, Queen Mary University of London, London, United Kingdom
- ⁷⁶ Department of Physics, Royal Holloway University of London, Surrey, United Kingdom
- ⁷⁷ Department of Physics and Astronomy, University College London, London, United Kingdom
- ⁷⁸ Laboratoire de Physique Nucléaire et de Hautes Energies, UPMC and Université Paris-Diderot and CNRS/IN2P3, Paris, France
- ⁷⁹ Fysiska institutionen, Lunds universitet, Lund, Sweden
- ⁸⁰ Departamento de Física Teórica C-15, Universidad Autónoma de Madrid, Madrid, Spain
- ⁸¹ Institut für Physik, Universität Mainz, Mainz, Germany
- ⁸² School of Physics and Astronomy, University of Manchester, Manchester, United Kingdom
- ⁸³ CPPM, Aix-Marseille Université and CNRS/IN2P3, Marseille, France
- ⁸⁴ Department of Physics, University of Massachusetts, Amherst MA, USA
- ⁸⁵ Department of Physics, McGill University, Montreal QC, Canada
- ⁸⁶ School of Physics, University of Melbourne, Victoria, Australia
- ⁸⁷ Department of Physics, The University of Michigan, Ann Arbor MI, USA
- ⁸⁸ Department of Physics and Astronomy, Michigan State University, East Lansing MI, USA
- ^{89a} INFN Sezione di Milano, Milano, Italy
- ^{89b} Dipartimento di Fisica, Università di Milano, Milano, Italy
- ⁹⁰ B.I. Stepanov Institute of Physics, National Academy of Sciences of Belarus, Minsk, Republic of Belarus
- ⁹¹ National Scientific and Educational Centre for Particle and High Energy Physics, Minsk, Republic of Belarus
- ⁹² Department of Physics, Massachusetts Institute of Technology, Cambridge MA, USA
- ⁹³ Group of Particle Physics, University of Montreal, Montreal QC, Canada
- ⁹⁴ P.N. Lebedev Institute of Physics, Academy of Sciences, Moscow, Russia
- ⁹⁵ Institute for Theoretical and Experimental Physics (ITEP), Moscow, Russia
- ⁹⁶ Moscow Engineering and Physics Institute (MEPhI), Moscow, Russia

- ⁹⁷ Skobeltsyn Institute of Nuclear Physics, Lomonosov Moscow State University, Moscow, Russia
- ⁹⁸ Fakultät für Physik, Ludwig-Maximilians-Universität München, München, Germany
- ⁹⁹ Max-Planck-Institut für Physik (Werner-Heisenberg-Institut), München, Germany
- ¹⁰⁰ Nagasaki Institute of Applied Science, Nagasaki, Japan
- ¹⁰¹ Graduate School of Science, Nagoya University, Nagoya, Japan
- ^{102a} INFN Sezione di Napoli, Napoli, Italy
- ^{102b} Dipartimento di Scienze Fisiche, Università di Napoli, Napoli, Italy
- ¹⁰³ Department of Physics and Astronomy, University of New Mexico, Albuquerque NM, USA
- ¹⁰⁴ Institute for Mathematics, Astrophysics and Particle Physics, Radboud University Nijmegen/Nikhef, Nijmegen, Netherlands
- ¹⁰⁵ Nikhef National Institute for Subatomic Physics and University of Amsterdam, Amsterdam, Netherlands
- ¹⁰⁶ Department of Physics, Northern Illinois University, DeKalb IL, USA
- ¹⁰⁷ Budker Institute of Nuclear Physics (BINP), Novosibirsk, Russia
- ¹⁰⁸ Department of Physics, New York University, New York NY, USA
- ¹⁰⁹ Ohio State University, Columbus OH, USA
- ¹¹⁰ Faculty of Science, Okayama University, Okayama, Japan
- ¹¹¹ Homer L. Dodge Department of Physics and Astronomy, University of Oklahoma, Norman OK, USA
- ¹¹² Department of Physics, Oklahoma State University, Stillwater OK, USA
- ¹¹³ Palacký University, RCPTM, Olomouc, Czech Republic
- ¹¹⁴ Center for High Energy Physics, University of Oregon, Eugene OR, USA
- ¹¹⁵ LAL, Univ. Paris-Sud and CNRS/IN2P3, Orsay, France
- ¹¹⁶ Graduate School of Science, Osaka University, Osaka, Japan
- ¹¹⁷ Department of Physics, University of Oslo, Oslo, Norway
- ¹¹⁸ Department of Physics, Oxford University, Oxford, United Kingdom
- ^{119a} INFN Sezione di Pavia, Pavia, Italy
- ^{119b} Dipartimento di Fisica Nucleare e Teorica, Università di Pavia, Pavia, Italy
- ¹²⁰ Department of Physics, University of Pennsylvania, Philadelphia PA, USA
- ¹²¹ Petersburg Nuclear Physics Institute, Gatchina, Russia
- ^{122a} INFN Sezione di Pisa, Pisa, Italy
- ^{122b} Dipartimento di Fisica E. Fermi, Università di Pisa, Pisa, Italy
- ¹²³ Department of Physics and Astronomy, University of Pittsburgh, Pittsburgh PA, USA
- ^{124a} Laboratório de Instrumentação e Física Experimental de Partículas—LIP, Lisboa, Portugal
- ^{124b} Departamento de Física Teórica y del Cosmos and CAFPE, Universidad de Granada, Granada, Spain
- ¹²⁵ Institute of Physics, Academy of Sciences of the Czech Republic, Praha, Czech Republic
- ¹²⁶ Faculty of Mathematics and Physics, Charles University in Prague, Praha, Czech Republic
- ¹²⁷ Czech Technical University in Prague, Praha, Czech Republic
- ¹²⁸ State Research Center Institute for High Energy Physics, Protvino, Russia
- ¹²⁹ Particle Physics Department, Rutherford Appleton Laboratory, Didcot, United Kingdom
- ¹³⁰ Physics Department, University of Regina, Regina SK, Canada
- ¹³¹ Ritsumeikan University, Kusatsu, Shiga, Japan
- ^{132a} INFN Sezione di Roma I, Roma, Italy
- ^{132b} Dipartimento di Fisica, Università La Sapienza, Roma, Italy

- ^{133a} INFN Sezione di Roma Tor Vergata, Roma, Italy
^{133b} Dipartimento di Fisica, Università di Roma Tor Vergata, Roma, Italy
^{134a} INFN Sezione di Roma Tre, Roma, Italy
^{134b} Dipartimento di Fisica, Università Roma Tre, Roma, Italy
^{135a} Faculté des Sciences Ain Chock, Réseau Universitaire de Physique des Hautes Energies—
Université Hassan II, Casablanca, Morocco
^{135b} Centre National de l’Energie des Sciences Techniques Nucleaires, Rabat, Morocco
^{135c} Université Cadi Ayyad, Faculté des sciences Semlalia Département de Physique, B.P. 2390
Marrakech 40000, Morocco
^{135d} Faculté des Sciences, Université Mohamed Premier and LPTPM, Oujda, Morocco
^{135e} Faculté des Sciences, Université Mohammed V, Rabat, Morocco
¹³⁶ DSM/IRFU (Institut de Recherches sur les Lois Fondamentales de l’Univers), CEA Saclay
(Commissariat a l’Energie Atomique), Gif-sur-Yvette, France
¹³⁷ Santa Cruz Institute for Particle Physics, University of California Santa Cruz, Santa Cruz
CA, USA
¹³⁸ Department of Physics, University of Washington, Seattle WA, USA
¹³⁹ Department of Physics and Astronomy, University of Sheffield, Sheffield, United Kingdom
¹⁴⁰ Department of Physics, Shinshu University, Nagano, Japan
¹⁴¹ Fachbereich Physik, Universität Siegen, Siegen, Germany
¹⁴² Department of Physics, Simon Fraser University, Burnaby BC, Canada
¹⁴³ SLAC National Accelerator Laboratory, Stanford CA, USA
^{144a} Faculty of Mathematics, Physics & Informatics, Comenius University, Bratislava, Slovak
Republic
^{144b} Department of Subnuclear Physics, Institute of Experimental Physics of the Slovak
Academy of Sciences, Kosice, Slovak Republic
^{145a} Department of Physics, University of Johannesburg, Johannesburg, South Africa
^{145b} School of Physics, University of the Witwatersrand, Johannesburg, South Africa
^{146a} Department of Physics, Stockholm University, Stockholm, Sweden
^{146b} The Oskar Klein Centre, Stockholm, Sweden
¹⁴⁷ Physics Department, Royal Institute of Technology, Stockholm, Sweden
¹⁴⁸ Department of Physics and Astronomy, Stony Brook University, Stony Brook NY, USA
¹⁴⁹ Department of Physics and Astronomy, University of Sussex, Brighton, United Kingdom
¹⁵⁰ School of Physics, University of Sydney, Sydney, Australia
¹⁵¹ Institute of Physics, Academia Sinica, Taipei, Taiwan
¹⁵² Department of Physics, Technion: Israel Inst. of Technology, Haifa, Israel
¹⁵³ Raymond and Beverly Sackler School of Physics and Astronomy, Tel Aviv University,
Tel Aviv, Israel
¹⁵⁴ Department of Physics, Aristotle University of Thessaloniki, Thessaloniki, Greece
¹⁵⁵ International Center for Elementary Particle Physics and Department of Physics, The
University of Tokyo, Tokyo, Japan
¹⁵⁶ Graduate School of Science and Technology, Tokyo Metropolitan University, Tokyo, Japan
¹⁵⁷ Department of Physics, Tokyo Institute of Technology, Tokyo, Japan
¹⁵⁸ Department of Physics, University of Toronto, Toronto ON, Canada
^{159a} TRIUMF, Vancouver BC, Toronto ON, Canada
^{159b} Department of Physics and Astronomy, York University, Toronto ON, Canada
¹⁶⁰ Institute of Pure and Applied Sciences, University of Tsukuba, Ibaraki, Japan

- ¹⁶¹ Science and Technology Center, Tufts University, Medford MA, USA
- ¹⁶² Centro de Investigaciones, Universidad Antonio Narino, Bogota, Colombia
- ¹⁶³ Department of Physics and Astronomy, University of California Irvine, Irvine CA, USA
- ^{164a} INFN Gruppo Collegato di Udine, Udine, Italy
- ^{164b} ICTP, Trieste, Udine, Italy
- ^{164c} Dipartimento di Fisica, Università di Udine, Udine, Italy
- ¹⁶⁵ Department of Physics, University of Illinois, Urbana IL, USA
- ¹⁶⁶ Department of Physics and Astronomy, University of Uppsala, Uppsala, Sweden
- ¹⁶⁷ Instituto de Física Corpuscular (IFIC) and Departamento de Física Atómica, Molecular y Nuclear and Departamento de Ingeniería Electrónica and Instituto de Microelectrónica de Barcelona (IMB-CNM), University of Valencia and CSIC, Valencia, Spain
- ¹⁶⁸ Department of Physics, University of British Columbia, Vancouver BC, Canada
- ¹⁶⁹ Department of Physics and Astronomy, University of Victoria, Victoria BC, Canada
- ¹⁷⁰ Waseda University, Tokyo, Japan
- ¹⁷¹ Department of Particle Physics, The Weizmann Institute of Science, Rehovot, Israel
- ¹⁷² Department of Physics, University of Wisconsin, Madison WI, USA
- ¹⁷³ Fakultät für Physik und Astronomie, Julius-Maximilians-Universität, Würzburg, Germany
- ¹⁷⁴ Fachbereich C Physik, Bergische Universität Wuppertal, Wuppertal, Germany
- ¹⁷⁵ Department of Physics, Yale University, New Haven CT, USA
- ¹⁷⁶ Yerevan Physics Institute, Yerevan, Armenia
- ¹⁷⁷ Domaine scientifique de la Doua, Centre de Calcul CNRS/IN2P3, Villeurbanne Cedex, France
- ¹⁷⁸ Also at Laboratório de Instrumentação e Física Experimental de Partículas—LIP, Lisboa, Portugal
- ¹⁷⁹ Also at Faculdade de Ciências and CFNUL, Universidade de Lisboa, Lisboa, Portugal
- ¹⁸⁰ Also at CPPM, Aix-Marseille Université and CNRS/IN2P3, Marseille, France
- ¹⁸¹ Also at TRIUMF, Vancouver BC, Canada
- ¹⁸² Also at Department of Physics, California State University, Fresno CA, USA
- ¹⁸³ Also at Faculty of Physics and Applied Computer Science, AGH-University of Science and Technology, Krakow, Poland
- ¹⁸⁴ Also at Department of Physics, University of Coimbra, Coimbra, Portugal
- ¹⁸⁵ Also at Università di Napoli Parthenope, Napoli, Italy
- ¹⁸⁶ Also at Institute of Particle Physics (IPP), Canada
- ¹⁸⁷ Also at Louisiana Tech University, Ruston LA, USA
- ¹⁸⁸ Also at Group of Particle Physics, University of Montreal, Montreal QC, Canada
- ¹⁸⁹ Also at Institute of Physics, Azerbaijan Academy of Sciences, Baku, Azerbaijan
- ¹⁹⁰ Also at Institut für Experimentalphysik, Universität Hamburg, Hamburg, Germany
- ¹⁹¹ Also at Manhattan College, New York NY, USA
- ¹⁹² Also at School of Physics and Engineering, Sun Yat-sen University, Guanzhou, China
- ¹⁹³ Also at Academia Sinica Grid Computing, Institute of Physics, Academia Sinica, Taipei, Taiwan
- ¹⁹⁴ Also at High Energy Physics Group, Shandong University, Shandong, China
- ¹⁹⁵ Also at California Institute of Technology, Pasadena CA, USA
- ¹⁹⁶ Also at Particle Physics Department, Rutherford Appleton Laboratory, Didcot, United Kingdom

¹⁹⁷ Also at Section de Physique, Université de Genève, Geneva, Switzerland

¹⁹⁸ Also at Departamento de Física, Universidade de Minho, Braga, Portugal

¹⁹⁹ Also at Department of Physics and Astronomy, University of South Carolina, Columbia SC, USA

²⁰⁰ Also at KFKI Research Institute for Particle and Nuclear Physics, Budapest, Hungary

²⁰¹ Also at Institute of Physics, Jagiellonian University, Krakow, Poland

²⁰² Also at Department of Physics, Oxford University, Oxford, United Kingdom

²⁰³ Also at DSM/IRFU (Institut de Recherches sur les Lois Fondamentales de l'Univers), CEA Saclay (Commissariat à l'Énergie Atomique), Gif-sur-Yvette, France

²⁰⁴ Also at Laboratoire de Physique Nucléaire et de Hautes Energies, UPMC and Université Paris-Diderot and CNRS/IN2P3, Paris, France

²⁰⁵ Also at Department of Physics, Nanjing University, Jiangsu, China

²⁰⁶ Deceased

References

- [1] Arnison G *et al* (UA1 Collaboration) 1984 Angular distributions and structure functions from two-jet events at the CERN SPS $p\bar{p}$ collider *Phys. Lett. B* **136** 294
- [2] Bagnaia P *et al* (UA2 Collaboration) 1984 Measurement of jet production properties at the CERN collider *Phys. Lett. B* **144** 283–90
- [3] Aaltonen T *et al* (CDF Collaboration) 2009 Search for new particles decaying into dijets in $p\bar{p}$ collisions at $\sqrt{s} = 1.96$ TeV *Phys. Rev. D* **79** 112002
- [4] Abazov V M *et al* (D0 Collaboration) 2009 Measurement of dijet angular distributions at $\sqrt{s} = 1.96$ TeV and searches for quark compositeness and extra spatial dimensions *Phys. Rev. Lett.* **103** 191803
- [5] ATLAS Collaboration 2010 Search for new particles in two-jet final states in 7 TeV proton–proton collisions with the ATLAS detector at the LHC *Phys. Rev. Lett.* **105** 161801
- [6] ATLAS Collaboration 2011 Search for quark contact interactions in dijet angular distributions in pp collisions at $\sqrt{s} = 7$ TeV measured with the ATLAS detector *Phys. Lett. B* **694** 327
- [7] Khachatryan V *et al* (CMS Collaboration) 2010 Search for dijet resonances in 7 TeV pp collisions at CMS *Phys. Rev. Lett.* **105** 211801
- [8] Khachatryan V *et al* (CMS Collaboration) 2010 Search for quark compositeness with the dijet centrality ratio in 7 TeV pp collisions *Phys. Rev. Lett.* **105** 262001
- [9] Khachatryan V *et al* (CMS Collaboration) 2011 Measurement of dijet angular distributions and search for quark compositeness in pp collisions at $\sqrt{s} = 7$ TeV *Phys. Rev. Lett.* submitted (arXiv:1102.2020 [hep-ex])
- [10] Cacciari M, Salam G P and Soyez G 2008 The anti- k_T jet clustering algorithm *J. High Energy Phys.* **JHEP04(2008)063**
- [11] Cacciari M and Salam G P 2006 Dispelling the n^3 myth *Phys. Lett. B* **641** 57
- [12] Adragna P *et al* 2010 Measurement of pion and proton response and longitudinal shower profiles up to 20 nuclear interaction lengths with the ATLAS tile calorimeter *Nucl. Instrum. Methods A* **615** 158–81
- [13] ATLAS Collaboration 2010 ATLAS calorimeter response to single isolated hadrons and estimation of the calorimeter jet scale uncertainty *CERN Report ATLAS-CONF-2010-052*
- [14] ATLAS Collaboration 2010 Jet energy scale and its systematic uncertainty in ATLAS for jets produced in proton–proton collisions at $\sqrt{s} = 7$ TeV *CERN Report ATLAS-CONF-2010-056*
- [15] ATLAS Collaboration 2011 Update on the jet energy scale systematic uncertainty for jets produced in proton–proton collisions at $\sqrt{s} = 7$ TeV measured with the ATLAS detector *CERN Report ATLAS-CONF-2011-007*
- [16] ATLAS Collaboration 2008 The ATLAS experiment at the CERN Large Hadron Collider *J. Instrum.* **3** S08003

- [17] ATLAS Collaboration 2010 Data-quality requirements and event cleaning for jets and missing transverse energy reconstruction with the ATLAS detector in proton–proton collisions at a center-of-mass energy of $\sqrt{s} = 7$ TeV *CERN Report* ATLAS-CONF-2010-038
- [18] Sjostrand T, Mrenna S and Skands P Z 2006 PYTHIA 6.4 physics and manual *J. High Energy Phys.* **JHEP05(2006)026**
- [19] ATLAS Collaboration 2010 ATLAS Monte Carlo tunes for MC09 *ATLAS Note* ATL-PHYS-PUB-2010-002
- [20] Sherstnev A and Thorne R S 2008 Parton distributions for LO generators *Eur. Phys. J. C* **55** 553
- [21] ATLAS Collaboration 2010 The ATLAS simulation infrastructure *Eur. Phys. J. C* **70** 823
- [22] Agostinelli S *et al* (GEANT4) 2003 GEANT4: a simulation toolkit *Nucl. Instrum. Methods A* **506** 250–303
- [23] Nagy Z 2002 Three-jet cross sections in hadron–hadron collisions at next-to-leading order *Phys. Rev. Lett.* **88** 122003
- [24] Nagy Z 2003 Next-to-leading order calculation of three-jet observables in hadron–hadron collisions *Phys. Rev. D* **68** 094002
- [25] Catani S and Seymour M H 1997 A general algorithm for calculating jet cross sections in NLO QCD *Nucl. Phys. B* **485** 291–419
- [26] Nadolsky P M *et al* 2008 Implications of CTEQ global analysis for collider observables *Phys. Rev. D* **78** 013004
- [27] Baur U, Hinchliffe I and Zeppenfeld D 1987 Excited quark production at hadron colliders *Int. J. Mod. Phys. A* **2** 1285
- [28] Baur U, Spira M and Zerwas P M 1990 Excited quark and lepton production at hadron colliders *Phys. Rev. D* **42** 815–24
- [29] Frampton P H and Glashow S L 1987 Chiral color: an alternative to the standard model *Phys. Lett. B* **190** 157
- [30] Frampton P H and Glashow S L 1987 Unifiable chiral color with natural GIM mechanism *Phys. Rev. Lett.* **58** 2168
- [31] Bagger J, Schmidt C and King S 1988 Axigluon production in hadronic collisions *Phys. Rev. D* **37** 1188
- [32] Pukhov A 2009 Calchep 3.2: MSSM, structure functions, event generation, batchs and generation of matrix elements for other packages arXiv:hep-ph/0412191v2
- [33] Randall L and Sundrum R 1999 A large mass hierarchy from a small extra dimension *Phys. Rev. Lett.* **83** 3370–3
- [34] Bijnens J, Eerola P, Maul M, Mansson A and Sjostrand T 2001 QCD signatures of narrow graviton resonances in hadron colliders *Phys. Lett. B* **503** 341
- [35] Aaltonen T *et al* (CDF Collaboration) 2007 Search for high-mass diphoton states and limits on Randall–Sundrum gravitons at CDF *Phys. Rev. Lett.* **99** 171801
- [36] Eichten E, Hinchliffe I, Kenneth Lane D and Quigg C 1984 Super collider physics *Rev. Mod. Phys.* **56** 579–707
- [37] Eichten E, Hinchliffe I, Kenneth Lane D and Quigg C 1986 *Rev. Mod. Phys.* **58** 1065–73 (erratum)
- [38] Chiappetta P and Perrottet M 1991 Possible bounds on compositeness from inclusive one jet production in Large Hadron Colliders *Phys. Lett. B* **235** 489–93
- [39] Meade P and Randall L 2008 Black holes and quantum gravity at the LHC *J. High Energy Phys.* **JHEP05(2008)003**
- [40] Anchordoqui L A, Feng J L, Goldberg H and Shapere A D 2004 Inelastic black hole production and large extra dimensions *Phys. Lett. B* **594** 363
- [41] Dai D *et al* 2008 BlackMax: a black-hole event generator with rotation, recoil, split branes and brane tension *Phys. Rev. D* **77** 076007
- [42] ATLAS Collaboration 2011 Measurement of jet production in proton–proton collisions at 7 TeV centre-of-mass energy with the ATLAS detector *Eur. Phys. J. C* **71** 1512
- [43] Aaltonen T *et al* (CDF Collaboration) 2009 Global search for new physics with 2.0 fb^{-1} at CDF *Phys. Rev. D* **79** 011101
- [44] Choudalakis G 2011 On hypothesis testing, trials factor, hypertests and the bump hunter arXiv:1101.0390

- [45] ATLAS Collaboration 2011 Luminosity determination in pp collisions and $\sqrt{s} = 7$ TeV using the ATLAS detector at the LHC *Eur. Phys. J* at press (arXiv: [1101.2185](#) [hep-ex])
- [46] Pumplin J *et al* 2002 New generation of parton distributions with uncertainties from global QCD analysis *J. High Energy Phys.* [JHEP07\(2002\)012](#)
- [47] Skands P Z 2009 The Perugia tunes arXiv:0905.3418
- [48] Lai H L *et al* (CTEQ Collaboration) 2000 Global QCD analysis of parton structure of the nucleon: CTEQ5 parton distributions *Eur. Phys. J. C* **12** 375–92
- [49] Junk T 1999 *Nucl. Instrum. Methods A* **434** 435
- [50] Gao J, Li C S, Wang J, Zhu H X and Yuan C-P 2011 Next-to-leading QCD effect to the quark compositeness search at the LHC *Phys. Rev. Lett.* **106** 142001